

University of Southern Queensland
Faculty of Health, Engineering & Sciences

**CIRCULAR GEOPOLYMER CONCRETE COLUMNS
WITH COMPOSITE REBARS**

A dissertation submitted by

Matthew Robertson

in fulfilment of the requirements of

ENG4111/ENG4112 Research Project

towards the degree of

Bachelor of Civil Engineering with Honours

Submitted: October, 2015

Abstract

Reinforced concrete (RC) is one of the most popular construction materials. Columns are critical to the safety as well as the performance of the structure. RC columns traditionally use Portland cement as a main ingredient for the cement as well as using steel bars and stirrups for reinforcement. One major problem encountered by RC columns is the corrosion of the reinforcement cages, which can result in deterioration of the concrete, loss of serviceability as well as, in extreme cases, brittle failure of the entire structure. This has resulted in the search for a product that will not corrode but still has similar behaviour. This search led to the trial of glass fibre reinforced polymer (GFRP) material, which is made from high strength glass fibres surrounded by polymer matrices and shaped in the form of bars, tubes and grids.

Another major problem is the issue of global warming. There is major concern over the amount of CO_2 released by Portland cement. Due to modern day societies being extremely environmentally conscientious, an alternative product is needed to reduce this. This has resulted in the product which is known as geopolymer cement. Geopolymer concrete has been used in many projects around the world, and has been found to have the same strength as concrete.

To test these two promising materials, six specimens were created, with the parameters of spacing between transverse reinforcement and type of transverse reinforcement varied. Each specimen was then tested through the application of axial loading with the internal longitudinal, internal transverse and external concrete strain recorded.

The obtained results stated that both GFRP hoop and spiral ties are effective in providing confinement to a GFRP reinforced geopolymer column. The results also show that the spiral ties are slightly more effective, due to having a higher ultimate load, ductility as well as confinement efficiency. These findings are why it is recommended that the spiral

ties be used if GFRP reinforced geopolymer concrete is to be used within the construction industry. This study differs from other studies as the effect of the longitudinal GFRP bars on the behaviour of the specimen has been included. It was calculated that the longitudinal bars resulted in an increase in strength between 6-9% of the entire specimen. This contribution from the longitudinal bars is not quite as much as the contribution of steel reinforcement (12%) however, are still significant enough to avoid being neglected. A theoretical analysis was also performed to find an accurate equation to predict the axial capacity of the specimens. It was found that the equation 5.5 shown in this report was the most accurate from existing literature. This equation does not result in an accurate prediction of the capacity of the specimens. This was due to the strength reduction factor (α_1) used being calculated for ordinary Portland cement concrete. An accurate prediction can be obtained if a strength reduction factor of 0.91 is used.

University of Southern Queensland
Faculty of Health, Engineering & Sciences

ENG4111/2 Research Project

Limitations of Use

The Council of the University of Southern Queensland, its Faculty of Health, Engineering & Sciences, and the staff of the University of Southern Queensland, do not accept any responsibility for the truth, accuracy or completeness of material contained within or associated with this dissertation.

Persons using all or any part of this material do so at their own risk, and not at the risk of the Council of the University of Southern Queensland, its Faculty of Health, Engineering & Sciences or the staff of the University of Southern Queensland.

This dissertation reports an educational exercise and has no purpose or validity beyond this exercise. The sole purpose of the course pair entitled “Research Project” is to contribute to the overall education within the student’s chosen degree program. This document, the associated hardware, software, drawings, and other material set out in the associated appendices should not be used for any other purpose: if they are so used, it is entirely at the risk of the user.

Dean

Faculty of Health, Engineering & Sciences

Certification of Dissertation

I certify that the ideas, designs and experimental work, results, analyses and conclusions set out in this dissertation are entirely my own effort, except where otherwise indicated and acknowledged.

I further certify that the work is original and has not been previously submitted for assessment in any other course or institution, except where specifically stated.

MATTHEW ROBERTSON

0061032821

Acknowledgments

I would like to take this opportunity to provide my thanks to the countless staff, lecturers, friends and family that have assisted myself in the completion of this project. I would however like to give special acknowledgement to the following people: Dr Allan Manalo, my on-campus supervisor for his constant support and guidance throughout this project, Ghingis Maranan, for his aid and technical support throughout this project, lastly I would like to thank Wayne Crowley and Martin Greach for their time and aid in the preparation and testing of the specimens.

With appreciation

MATTHEW ROBERTSON

Contents

Abstract	i
Acknowledgments	v
List of Figures	xi
List of Tables	xvi
Chapter 1 Introduction	1
1.1 Background and Problem Definition	1
1.2 Research Significance and Scope of the Project	3
1.3 Research Objectives	3
1.4 Specimen Details	4
1.5 Structure of the Dissertation	5
Chapter 2 Literature Review	7
2.1 Introduction	7
2.2 Geopolymer Concrete Behaviour and Benefits	7
2.3 GFRP Composite Material	9

2.3.1	Axial tensile strength	11
2.3.2	Compressive strength	12
2.3.3	Shear strength	13
2.3.4	Bond strength	13
2.3.5	Bend strength	14
2.4	Effect of Confinement of Concrete Columns	15
2.4.1	External Confinement	15
2.4.2	Internal Confinement	17
2.5	Factors Influencing the Axial Capacity	18
2.5.1	Longitudinal Reinforcement Ratio (ρ_{st})	19
2.5.2	Horizontal Reinforcement Ratio (ρ_s)	20
2.5.3	Column Dimensions	21
2.5.4	Eccentricity	22
2.5.5	Concrete Strength	23
2.5.6	Transverse Reinforcement Yield Strength	24
2.6	Theoretical Modelling GFRP Reinforced Geopolymer Concrete	24
2.7	Summary	26
Chapter 3 Materials and Methodology		28
3.1	Introduction	28
3.2	Material Properties	28
3.2.1	Geopolymer Concrete	28

3.2.2	GFRP Reinforcement	29
3.3	Specimen Details	30
3.4	Specimen Preparation	34
3.5	Instrumentation & Test Setup	37
3.6	Summary	40
Chapter 4 Results and Observations		41
4.1	Introduction	41
4.2	Load vs Deformation Behaviour	41
4.3	Behaviour of the C1-0 Specimen	42
4.4	Behaviour of the C1-50 Specimen	44
4.5	Behaviour of the C1-100 Specimen	48
4.6	Behaviour of the C1-200 Specimen	52
4.7	Behaviour of the S1-50 Specimen	54
4.8	Behaviour of the S1-100 Specimen	58
4.9	Conclusion	61
Chapter 5 Discussion of Results and Effect of the Test Variable		62
5.1	Introduction	62
5.2	Effect of Spacing	63
5.2.1	Spacing of Hoop Ties	63
5.2.2	Spacing of Spiral Ties	69

5.2.3	Summary of the Effect of Spacing	74
5.3	Effect of Type of Transverse Reinforcement	75
5.3.1	Spacing of 50mm	75
5.3.2	Spacing of 100mm	79
5.3.3	Summary of the Effect of the Type of Transverse Reinforcement	84
5.4	Theoretical Analysis	85
5.5	Conclusion	87
Chapter 6 Summary, Conclusions and Recommendation for Future Work		88
6.1	Summary	88
6.2	Conclusions	90
6.2.1	Spacing of Transverse Reinforcement	90
6.2.2	Type of Transverse Reinforcement	90
6.2.3	General Conclusions Reached From Experimental Results	90
6.2.4	Theoretical Analysis	91
6.3	Recommendations for Future Work	91
References		92
Appendix A Project Specification		96
Appendix B Risk Management Plans		99
Appendix C Instrumentation Used During Testing		110

List of Figures

2.1	The basic material composition of FRP products.	10
2.2	The preparation of the GFRP of the axial tensile strength.	11
2.3	The setup of a bond test using GFRP reinforcement and geopolymer concrete. 14	
2.4	The test setup of a bend strength test.	15
2.5	Concrete externally confined by a GFRP wrap.	16
2.6	Theoretical stress-strain plot of confined concrete vs. unconfined concrete. 18	
2.7	The effect of the longitudinal reinforcement on ductility	19
2.8	Reinforcement details for specimens.	21
2.9	Test column reinforcing details.	22
2.10	Effect of concrete strength on the axial capacity of confined concrete. . . . 24	
3.1	GFRP bars.	30
3.2	The spiral and circular ties used as transverse reinforcement.	30
3.3	The top view of all specimens.	31
3.4	The design of the 1m specimens reinforced by circular ties.	32
3.5	The design of the 1m specimens restrained by a continuous spiral.	33

3.6	The constructed reinforcement cages.	34
3.7	The attachment of the internal strain gauges.	34
3.8	The concrete spacers.	35
3.9	The formworks used for casting the specimens.	36
3.10	The internal configuration of each specimen.	36
3.11	The casting of the concrete.	37
3.12	The setup of the instrumentation and specimen for testing	38
3.13	The setup of each specimen.	39
4.1	The deformation of all specimens.	42
4.2	Core crushing failure of specimen C1-0.	43
4.3	Load vs Longitudinal Strain for the C1-0 specimen.	43
4.4	Load vs Concrete Strain for the C1-0 specimen.	44
4.5	Core crushing failure of the C1-50 specimen.	45
4.6	Load vs Longitudinal Strain for the C1-50 specimen.	45
4.7	Load vs Transverse Strain for the C1-50 specimen.	46
4.8	Load vs Concrete Strain for the C1-50 specimen.	46
4.9	Bending of the longitudinal bars.	47
4.10	Longitudinal bars extruding from the base.	48
4.11	Cracking of the patched area.	48
4.12	Shear failure of the C1-100 specimen.	49
4.13	Load vs Longitudinal Strain for the C1-100 specimen.	49

4.14	Load vs Transverse Strain for the C1-100 specimen.	50
4.15	Load vs Concrete Strain for the C1-100 specimen.	50
4.16	Splitting of the longitudinal bars and seperation of circular ties for the C1-100 specimen.	51
4.17	Shear failure of specimen C1-200.	52
4.18	Load vs Longitudinal Strain for the C1-200 specimen.	52
4.19	Load vs Transverse Strain for the C1-200 specimen.	53
4.20	Load vs Concrete Strain for the C1-200 specimen.	53
4.21	core crushing of the S1-50 specimen.	55
4.22	Load vs Longitudinal Strain for the S1-50 specimen.	55
4.23	Load vs Transverse Strain for the S1-50 specimen.	56
4.24	Load vs Concrete Strain for the S1-50 specimen.	56
4.25	The extrusion of longitudinal bars of the specimen S1-50 from the top of the specimen (left) as well as the base (right).	57
4.26	The core crushing of specimen S1-100.	58
4.27	Load vs Longitudinal Strain for the S1-100 specimen.	58
4.28	Load vs Transverse Strain for the S1-100 specimen.	59
4.29	Load vs Concrete Strain for the S1-100 specimen.	59
4.30	The buckling of the longitudinal bars.	60
4.31	The splitting of the vertical bars.	61
5.1	The average strain carried by the longitudinal bars transversely reinforced by hoop ties.	63

5.2	The average strain carried by the transverse hoop ties.	64
5.3	The compressive deflection of the specimens reinforced with hoop ties. . .	65
5.4	The mid-span expansion of the C1-0 specimen.	66
5.5	The mid-span expansion of the C1-50 specimen.	66
5.6	The mid-span expansion of the C1-100 specimen.	67
5.7	The mid-span expansion of the C1-200 specimen.	67
5.8	The average strain carried by the longitudinal bars transversely reinforced by spiral ties.	69
5.9	The average strain carried by spiral ties.	70
5.10	The compressive deflection of the specimens reinforced with a spiral tie. .	71
5.11	The mid-span expansion of the C1-0 specimen.	72
5.12	The mid-span expansion of the S1-50 specimen.	72
5.13	The mid-span expansion of the S1-100 specimen.	73
5.14	The strain carried in the longitudinal bars of specimens that had a spacing of 50mm.	75
5.15	The strain carried in the transverse reinforcement of specimens that had a spacing of 50mm.	76
5.16	The compressive deflection of the specimens reinforced with a spacing of 50mm.	77
5.17	The mid-span expansion of the C1-0 specimen.	77
5.18	The mid-span expansion of the C1-50 specimen.	78
5.19	The mid-span expansion of the S1-50 specimen.	78

5.20	The strain carried in the longitudinal bars of specimens that had a spacing of 100mm.	80
5.21	The strain carried in the transverse reinforcement of specimens that had a spacing of 100mm.	80
5.22	The compressive deflection of the specimens reinforced with a spacing of 100mm.	81
5.23	The mid-span expansion of the C1-0 specimen.	82
5.24	The mid-span expansion of the C1-100 specimen.	82
5.25	The mid-span expansion of the S1-100 specimen.	83
C.1	The 2000kN hydraulic jack used.	112
C.2	The circular plate used to evenly distribute the load.	112
C.3	The neoprene rubber used.	113
C.4	The steel plate that was used.	113
C.5	The load cell used.	114
C.6	The base plate used.	114
C.7	The stringpot used to measure deflection.	115
C.8	The lasers used to measure the mid span expansion.	115
C.9	The aviary wire used to control shattered concrete.	116
C.10	The computer used to log all recorded data.	117

List of Tables

1.1	Column Specimens	5
2.1	Applications of Geopolymeric Material Based on Si:Al Atomic Ratio . . .	8
2.2	The usual tensile properties of GFRP bars.	12
2.3	Mechanical properties of ASLAN GFRP bars produced by Hughes Brothers Inc.	12
2.4	Mechanical properties of V-ROD GFRP bars produced by Pultrall Inc. . .	12
2.5	Summary of column tests.	23
3.1	Tested Properties of geopolymer concrete used.	29
3.2	Mechanical properties of GFRP reinforcement.	30
3.3	Specimen Details	31
5.1	The percentage increase in strength contributed by the longitudinal bars for specimens with hoop ties.	68
5.2	The percentage increase in strength contributed by the longitudinal bars for specimens with spiral ties.	74
5.3	The percentage increase in strength contributed by the longitudinal bars for specimens with a spacing of 50mm.	79

5.4 The percentage increase in strength contributed by the longitudinal bars
for specimens with a spacing of 100mm. 84

5.5 The results that were obtained through the use of equations 5.2-5.5. 86

5.6 The results yielded through different α_1 values. 86

Chapter 1

Introduction

1.1 Background and Problem Definition

Reinforced concrete (RC) is one of the most popular construction materials. Columns are vertical members used in construction to support compressive loads and moments applied from higher levels. These vertical members are critical to the safety as well as the performance of the structure. RC columns traditionally use Portland cement as a main ingredient for the cement as well as using steel bars and stirrups for reinforcement. One major problem encountered by RC columns is the corrosion of the reinforcement cages. The corrosion of the steel cages can result in deterioration of the concrete, loss of serviceability as well as, in extreme cases, brittle failure of not only the column but the entire structure. Many environmental conditions, including moisture, marine conditions and freeze-thaw, increase the rate of the corrosion process, which results in a rapid decrease of the life expectancy. The cost of repairing this corrosion can be at least twice the cost of the original project. This has resulted in the search for a product that will not corrode but still has the same effect on the strength and behaviour of the RC column. This search led to the trial of fibre reinforced polymer (FRP) material. At the current point in time there are two (2) types of FRP materials that are used in industry. These types are carbon fibre reinforced polymers (CFRP) as well as glass fibre reinforced material (GFRP), which has started to become popular within Australia. GFRP is made from high strength glass fibres surrounded by polymer matrices and shaped in the form of bars, tubes and grids in a large variety of shapes and characteristics.

The behaviour of FRP has been the subject of numerous studies. These studies, however, have not tested the compressive behaviour of GFRP bars with lateral reinforcement. Having an understanding of this behaviour will allow GFRP products to be used within compression members. As Australia currently does not have a standard for the use of FRP products, this study will recommend changes to AS 3600-2009 to allow use within Australia by comparing tested results with theoretical results obtained by using the existing standard.

Another major problem is the issue of global warming. There is major concern over the amount of CO_2 released by Portland cement during the curing process. Studies have shown that the cement industry is responsible for approximately 6% of CO_2 emissions (McCaffery 2002). Due to modern day societies being extremely environmentally conscientious, an alternative product is needed to reduce this amount. Although the use of Portland cement is still unavoidable for the predictable future, there are many studies underway to find a suitable product serve as a replacement. Until this product is found, multiple materials are being used in an effort to decrease the amount of Portland cement. This has resulted in the product which is known as geopolymer cement. Geopolymer concrete has been used in many projects around the world, and has been found to have the same strength as concrete. However few studies have investigated the behaviour of reinforced geopolymer concrete (RGC) members.

Although geopolymer concrete is becoming increasingly popular within the Australian industry, the properties of geopolymer concrete have never been tested with the use of GFRP reinforcement. This research will therefore test the behaviour of GFRP RGC. As such there is a lack of knowledge of the behaviour of GFRP reinforced concrete within compression. This lack of knowledge has resulted in the recommendation that GFRP should not be used within compressive members. There have however been several studies that investigate the use of GFRP reinforced members within compression. These studies have found that GFRP acts as a suitable reinforcement to steel reinforcement for confining concrete (Tobbi, Farghaly & Benmokrane 2012). To address this problem, experimental research will be conducted, with the results recorded and compared to a theoretical analysis using suitable codes for concrete structures.

1.2 Research Significance and Scope of the Project

Understanding the behaviour of geopolymer concrete members reinforced with GFRP bars and stirrups has been objective of multiple research efforts internationally. The flexural and shear behaviour has been the main topic of such research however, and as such, the level of understanding has significantly increased to the point where many standards and codes have been developed. There have been very few studies on the use of GFRP as vertical and lateral reinforcement within members under compression. Having additional understanding of the compressive behaviour of GFRP would result in a larger variety of applications within compression members. As Australia is one country that does not have a standard or code for using GFRP reinforcement, due to its scarce use within Australian industry, this study will compare the results that are obtained against AS 3600-2009 Concrete Structures, as well as recommending changes that should be made if GFRP is to be correctly used within industry in Australia.

Despite geopolymer concrete's increase in popularity within industry, the properties of geopolymer concrete have never before been tested with GFRP reinforcement. There is also very limited knowledge on the behaviour of GFRP in compression. Therefore the aim of this research is to investigate the behaviour of GFRP RGC.

The scope of this study consists of experimental as well as theoretical components. The experimental component will investigate the compressive behaviour of GFRP RGC columns through the design, construction and testing of six full scale columns. The effect of a variety of parameters such as: longitudinal reinforcement ratio, spacing of stirrups, and confinement configuration were also investigated. The theoretical component aims to determine revisions that will account for the behaviour of GFRP reinforcements that must be made to the current compression design requirements.

1.3 Research Objectives

The objectives of this research are therefore:

1. Research the use and parameters of geopolymer concrete and GFRP and their suitability to be used as an alternative to steel reinforced concrete.

2. Investigate, through testing, the effects of different transverse reinforcement types on the overall strength and behaviour of the specimen.
3. Investigate, through testing, the effect of GFRP ties spacing or pitch on the strength and behaviour of the specimen, as well as analysing the type of failure.
4. Theoretically predict the behaviour of the specimens using equations from existing literature.

The parameters of GFRP bars are being investigated to determine the compressive behaviour of these bars, as well as their suitability for use within geopolymer concrete structures under compressive loads. The design of transverse reinforcement is being investigated to determine the effect that different designs will have on the strength and behaviour of geopolymer concrete members under compressive loading. The spacing of the transverse reinforcement will also be investigated to determine the effect of the spacing on not only the strength and behaviour of the specimen, but also the mode of failure of the column. A key component of this research is to compare the obtained results to the current standard used in Australia for RC design, AS 3600-2009. This standard covers the use of steel reinforcement in concrete members. Therefore, recommendations will be made to alter the code to accommodate for not only GFRP reinforcement but to also account for the use of geopolymer concrete.

Before any construction or testing was conducted, a Risk Management Plan (RMP) was performed, with a copy of these RMPs supplied in Appendix B.

1.4 Specimen Details

To achieve the previously mentioned objectives, analytical and experimental programs were created and then conducted. The experimental phase comprised of the construction of six GFRP reinforced geopolymer concrete columns that were 250mm in diameter and 1000mm in height. Each column had a varied pitch or spacing for the spiral or hoop tie stirrups, with the setup as seen below in table 1.1. The name of each specimen was defined as X#-spacing, where: X is the reinforcement type, S for Spiral and C for Hoop ties; # is the height of the specimen in metres; and spacing is the spacing between the reinforcement.

Table 1.1: Column Specimens

Specimen	Reinforcement Type	Height (m)	Spacing (mm)
C1-0	None	1	0
C1-50	Hoop Ties	1	50
C1-100	Hoop Ties	1	100
C1-200	Hoop Ties	1	200
S1-50	Spiral	1	50
S1-100	Spiral	1	100

This study proposed to test the following parameters: longitudinal reinforcement ratio, slenderness ratio, spacing of stirrups, and confinement configuration.

1.5 Structure of the Dissertation

This dissertation will consist of 7 chapters, tables, figures, symbols and references. The contents of each chapter are provided below:

Chapter 1: This chapter provides an overview of RC columns use within the construction industry along with defining the problems associated with their use within industry. The scope of the project along with the objectives of the study are presented along with the methodology used. The structure of the dissertation is also presented.

Chapter 2: This chapter contains a literature review concerning: the production, use, benefits and behaviour of geopolymer concrete; a full historical review that covers all previous work on GFRP, along with all properties of GFRP bars and stirrups; the effect of confinement on concrete columns, factors that influence the column bearing capacity, numerical confinement modelling of circular RC columns, as well as the current equations for predicting the axial capacity of RC columns in compression within the design codes and guidelines available from North America and Australia, namely AS 3600-2009, ACI440.1R-06, CSA S6-06 and CAN/CSA S806-12.

Chapter 3: This chapter will discuss the experimental research program, specimen details, used materials, test procedure, test set up along with measuring devices.

Chapter 4: This chapter will provide an overview of the testing objectives and the experimental program, as well as displaying the results of the experimental program.

Chapter 5: This chapter will discuss the obtained results as well as analysing the effect of test variable on the overall behaviour of the GFRP GRC column specimens. This chapter will also compare the observed results to expected values from existing literature

Chapter 6: This chapter includes a summary of the research as well as providing overall conclusions based on both the theoretical and experimental results obtained throughout the duration of the study. Recommendations for future work have also been provided.

Chapter 2

Literature Review

2.1 Introduction

This chapter of the dissertation covers any research on not only GFRP and geopolymer concrete but as well as the test parameters, such as confinement and bearing capacity, while also investigating the current standards for concrete structures within Australia, America as well as in Canada.

2.2 Geopolymer Concrete Behaviour and Benefits

A major problem within modern society is the issue of global warming. There is major concern over the amount of CO_2 released by Portland cement during the curing process. Studies have shown that the cement industry is responsible for approximately 6% of CO_2 emissions (McCaffery 2002). Due to modern day societies being extremely environmentally conscientious, an alternative product is needed to reduce this amount. Although the use of Portland cement, the main ingredient in concrete, is still unavoidable for the predictable future, there are many studies underway to find a suitable product serve as a replacement. Geopolymer concrete has been created as a way of reducing the amount of CO_2 produced. Geopolymer concrete reduces the carbon emissions but approximately 60-70% compared to concrete using Portland cement as a main ingredient (Wagners 2012). This converts to approximately 184 kg of CO_2 for every m^3 of 32 MPa geopolymer concrete.

Geopolymers have two main components, being the source materials and the alkaline liquids (Wallah & Ramgam 2006). The source materials used should have a high level of silicon and aluminium, such as minerals like: kaolinite, clays, spinel, andalusite as well as micas; however, by products such as fly ash, red mud, silica fume, rice-husk ash and slag are all suitable products. Soluble alkali metals, usually based from sodium or potassium, are the preferred materials for use as alkaline liquids.

The ratio of silicon to aluminium also determines the application that would be best suited to the geopolymeric material, as seen below in table 2.1.

Table 2.1: Applications of Geopolymeric Material Based on Si:Al Atomic Ratio
(Wallah & Ramgam 2006)

Si:Al ratio	Applications
1	-Bricks -Ceramics -Fire protection
2	-Low CO_2 cements and concretes -Radioactive and toxic waste encapsulation
3	-Fire protection fibre glass composite -Foundry equipments -Heat resistant composites, 200°C to 1000°C -Tooling for aeronautics titanium process
> 3	-Sealants for industry, 200°C to 600°C -Tooling for aeronautics SPF aluminium
20 - 35	-Fire resistant and heat resistant fibre composites

In Australia, geopolymers have been used in the development of railway sleepers, sewer pipelines, building products, shotcrete, wall panels, high performance fibre reinforced laminates, protective coatings, masonry materials as well as repair materials (Wallah & Ramgam 2006).

Previous laboratory studies have shown that geopolymer concrete can experience rapid hardening at room temperature, while gaining a compressive strength of approximately 20 MPa at a temperature of 20° after 4 hours, while reaching strengths of 70-100 MPa at the completion of 28 days (Wallah & Ramgam 2006). Further tests also found that geopolymer concrete was superior in heat and fire resistance test as well. While Portland

cement tends to experience a rapid drop in compressive strength at approximately 300°, the compressive strength of the geopolymer cements tested was stable up to 600°.

Geopolymer concrete has been found to have: the same or better tensile, flexural and compressive strength, better fire and chemical resistance, high early strength development, durable, lower creep and shrinkage, comparable or lower modulus of elasticity, as well as similar behaviour, elastic properties and failure mode to concrete made from ordinary Portland cement (Akhilesh, Marepally & Padmakanth 2015).

Acid resistance is also another major benefit of geopolymer cement. Due to its lime content, Portland cement can easily be affected by the smallest amount of acid. Testing has shown that when Portland cement and geopolymer cement specimens were exposed to 5% of sulphuric acid and chloric acid, Portland cement lost between 30 to 60 % of its initial weight while the geopolymer cement lost only 5 to 8 % of the initial weight (Davidovits 1994). Despite having a higher alkali content, geopolymer concrete has been found to not create a dangerous Alkali-Aggregate-Reaction, where this event can occur frequently within Portland cement.

2.3 GFRP Composite Material

Fibre reinforced polymer, (FRP), is a combination of multiple materials that yields a product that is more effective than its elements; that is generally made of a fibre material that is bound by a resin. Glass fibre reinforced polymers (GFRP) are a structural reinforcing bar made from high strength and corrosion resistant glass fibres that are wrapped by an extremely durable polymeric epoxy resin (Iran 2015), an example of GFRP is shown below in figure 2.1.

GFRP has numerous advantages over steel when it comes to use as reinforcement in concrete. GFRP has a high tensile strength, high chemical resistance, excellent insulating properties as well as being a cheap material that is also non corrosive (P.K.Mallick 2007). GFRP does however have its disadvantages however, being: a high density and hardness, along with a low tensile modulus, sensitivity to abrasion during handling and a relatively low fatigue resistance.

GFRP has uses in a large variety of situations within the construction industry (Hughes Brothers

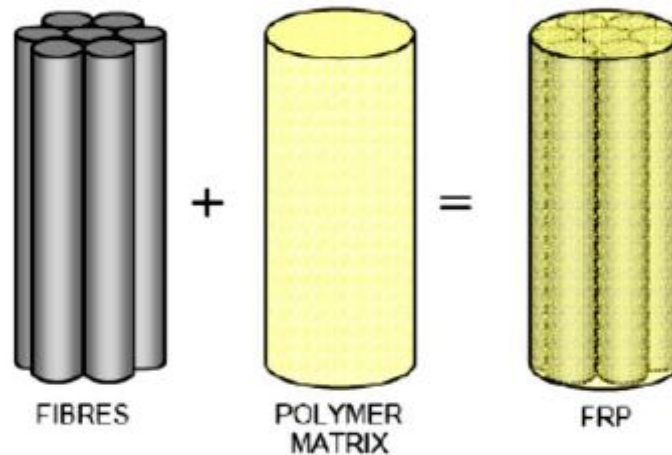


Figure 2.1: The basic material composition of FRP products.

(Affi 2013)

2011). These situations include:

- Concrete Exposed to De-Icing Chlorides
- Concrete Exposed to Marine Chlorides
- Concrete Exposed to High Voltages & Electromagnetic Fields
- Concrete Susceptible to Corrosion
- Tunnelling & Mining
- Masonry Strengthening & Historic Preservation

GFRP has many desirable properties, such as a high strength to weight ratio, high stiffness to weight ratio, high energy absorption, high performance, along with outstanding fatigue damage and corrosion, which are used within civil engineering infrastructure. Due to this variety of applications, the use of GFRP reinforcement within concrete structures is strongly swayed by both the mechanical and physical properties. The mechanical properties of GFRP provide benefits to the product that they are used within. This section aims to provide insight to not only the testing methods used to determine these properties but also mechanical properties of GFRP reinforcement bars such as:

- Axial tensile strength

- Compressive strength
- Shear strength
- Bond strength
- Bend portion strength

2.3.1 Axial tensile strength

In order to determine the axial tensile strength of GFRP bars, a universal testing machine (UTM) should be used (You, Park, Deo & Hwang 2014). In order to test this, the GFRP bar should be inserted into steel grips, with stoppers installed at opposite ends. The space between the rebar and steel grip should be filled with mortar that is resistant to shrinkage. A screw was placed at each end of the specimen so that the rebar could be fixed to a nut, as seen in figure 2.2 below. The loading is then applied with the observed results recorded.

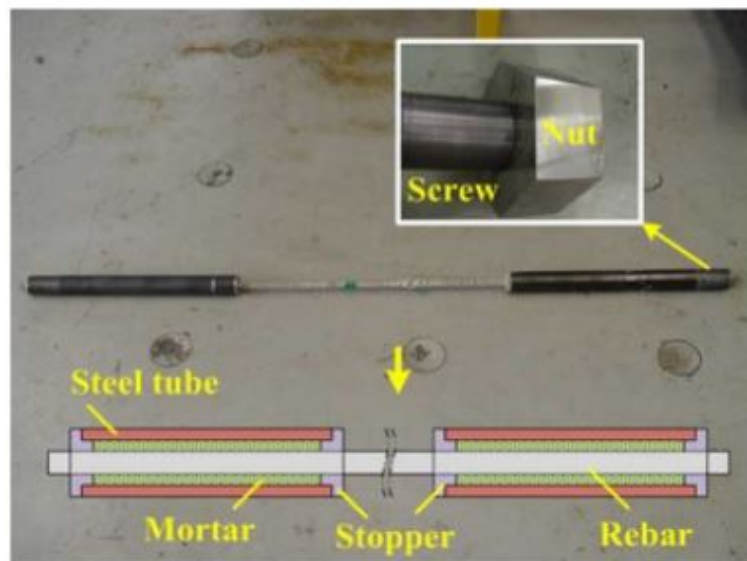


Figure 2.2: The preparation of the GFRP of the axial tensile strength.

Most manufacturers provide a copy of the expected tensile strength of their GFRP products, with some shown below in tables 2.2-2.4 show the expected tensile strength and modulus of elasticity provided by not only GFRP manufacturers but also standards.

Table 2.2: The usual tensile properties of GFRP bars.

(ACI 2006)	Tensile Strength (MPa)	483-1600
	Elastic Modulus (GPa)	35.0-51.0
	Rupture Strain (%)	1.9-4.4

Table 2.3: Mechanical properties of ASLAN GFRP bars produced by Hughes Brothers Inc.

(Hughes Brothers 2011)

Size	2	3	4	5	6	7	8	9	10
Diameter (mm)	6	10	13	16	19	22	25	29	32
Area (mm^2)	31.67	71.26	126.7	197.9	285.0	387.9	506.7	641.3	791.7
Tensile Strength (MPa)	896	827	758	724	690	655	620	586	551
Ultimate Tensile Load (kN)	28.3	58.7	95.9	143.4	196.6	254	314.3	375.8	436.6
Modulus of Elasticity (GPa)	46	46	46	46	46	46	46	46	46
Ultimate Strain (%)	1.94	1.79	1.64	1.57	1.49	1.42	1.34	1.27	1.19

Table 2.4: Mechanical properties of V-ROD GFRP bars produced by Pultrall Inc.

(Pultrall 2015)

Trade Name	Tensile Strength (MPa)	Modulus of Elasticity (GPa)	Tensile Strain (%)
V-Rod LM	880-960	42.5 ± 2.5	2.07-2.26
V-Rod Standard	800-1140	52.5 ± 2.5	1.52-2.17
V-Rod HM	1000-1372	62.6 ± 2.5 - 66.4 ± 2.5	1.51-2.11

2.3.2 Compressive strength

Due to a large variety of failure modes (ACI 2006), there is no standard compression test for GFRP composites. The standard mode of failure is buckling, however this can range from buckling of the entire specimen to the buckling of only the fibres. Testing of the compressive behaviour of GFRP bars leads to inaccurate measurements due to the non-homogenous nature of the GFRP materials, along with the occurrence of micro buckling of fibres. A standard testing procedure is yet to be developed due to this occurrence, however Deitz suggests that the compressive strength should be equal to approximately 50% of the ultimate tensile strength for GFRP bars (Deitz, Harik & Gesund 2013).

2.3.3 Shear strength

Due to the way GFRP bars are created, most have a low resistance to shear. This is due to the resin that exists between the fibres and as there is also no reinforcement between layers, the shear strength is normally controlled by the resin, which is normally made of a weaker material. Compared to steel, concrete that uses GFRP as sheer reinforcement tends to have a higher deflection as well as wider cracks before failure (Farahmand 1996). This is due to GFRP bars having a significantly lower modulus of elasticity when compared to steel (200GPa).

2.3.4 Bond strength

The aim of a direct pullout test is to determine the bond between the reinforcement bar and concrete. A typical direct pullout test is shown below in figure 2.3. The depth that the bar is cast into the concrete block is normally varied. The failure load and mode of failure is normally recorded (Maranan, Manalo, Karunasena & Benmokrane 2015). The bond stress is then calculated using equation 2.1.

$$\mu = \frac{P}{\pi \times l_e \times d_b} \quad (2.1)$$

In equation 2.1, μ refers to the bond stress, P is the maximum load applied, l_e is the embedded length of the bar and d_b is the diameter of the bar (Hossain, Ametrano & Lachemi 2014). The failure between GFRP tends to occur in one of two methods, being: pullout and splitting of the concrete. Pullout failure tends to occur when the embedded bar length is small, or the concrete is well confined or has a large cover. Likewise, a small concrete cover and/or unconfined concrete normally results in splitting of the concrete, which is the most common form of failure within steel reinforced concrete used within practical based applications (Afifi 2013).

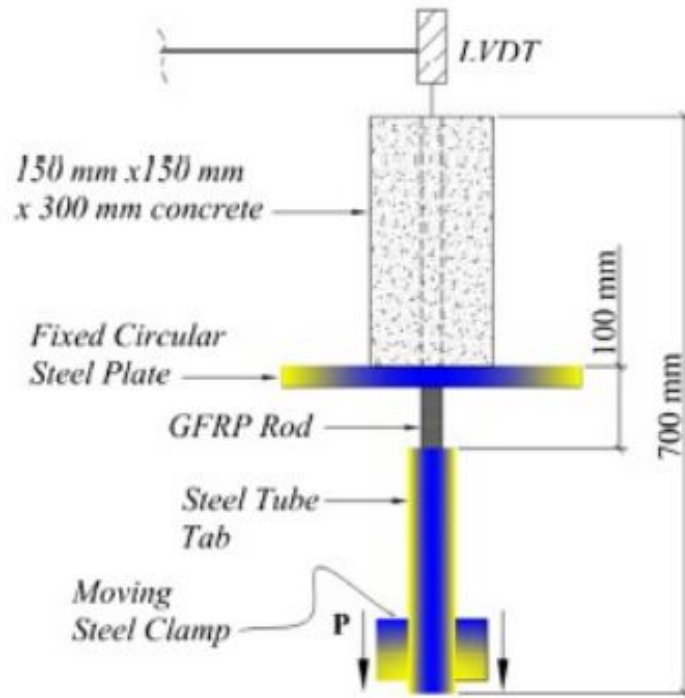


Figure 2.3: The setup of a bond test using GFRP reinforcement and geopolymer concrete.

(Maranan et al. 2015)

2.3.5 Bend strength

There are many applications within the civil engineering industry that call for the use of bent GFRP bars (Hughes Brothers 2015). The portion of the bar that is bent will result in substantial drop in the tensile strength, up to 62 % in some cases. The Canadian standard (CSA 2012) refers to using the B.5 method to test the strength of GFRP bars and stirrups. A typical setup of this method is shown below in figure 2.4. This test consists of a GFRP stirrup being cast between two steel reinforced concrete blocks. A hydraulic jack is then placed between the two blocks, with a load, aims to break the stirrup at the bent position within a 10 minute time limit, applied and recorded. The failure load is then placed into equation 2.2, below, to calculate the bend strength.

$$f_{bend} = \frac{P}{2 \times A_b} \quad (2.2)$$

Where f_{bend} is the bend strength in MPa, P is the failure load in N and A_b is the cross-sectional area of the GFRP stirrup in mm^2 .

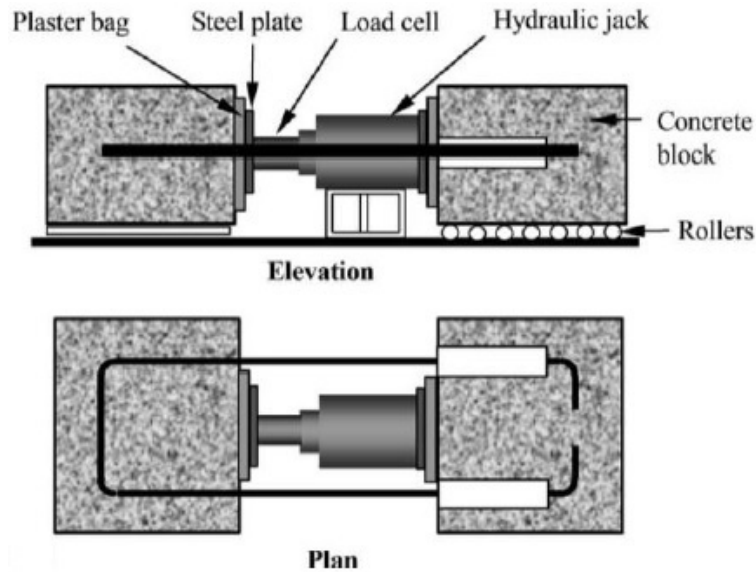


Figure 2.4: The test setup of a bend strength test.

(Afifi 2013)

2.4 Effect of Confinement of Concrete Columns

Confinement aims to significantly increase the ductility and strength of concrete (Deb 2015). Confinement pressure results in a higher failure load by restricting the expansion of the specimen and the growth of tensile cracks. This can be obtained by confining the concrete externally or internally. External confinement relies on the use of tubes to provide a lateral pressure on the column. Internal confinement uses the spacing of transverse reinforcement to increase the failure load and prevent crack control.

2.4.1 External Confinement

The main aim of externally confining concrete is to reduce the effect of the concrete members brittle behaviour. Externally confined concrete involves the member being wrapped in a fabric that aims to reduce expansion and tensile cracks, while creating a higher failure load by applying confining pressure. This confining pressure allows the member to carry higher loads than an unreinforced column could take. A standard setup of externally confined concrete is shown below in figure 2.5.

Concrete can be externally confined through the use of steel tubes, FRP tubes, as well as a GFRP wrap, which is only used for testing specimens. The use of steel tubes has been

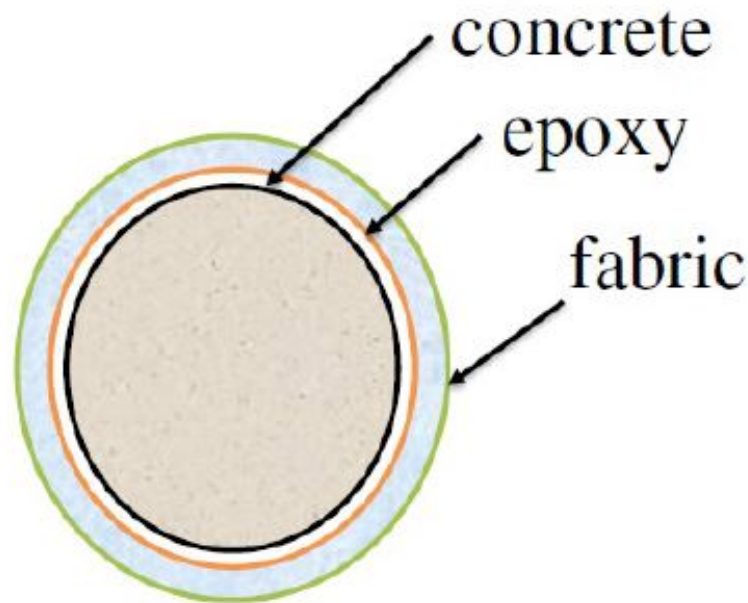


Figure 2.5: Concrete externally confined by a GFRP wrap.

(Deb 2015)

has become an effective solution to problems faced within the civil engineering industry (Zeghiche & Chaoui 2005). Concrete filled steel tubes are economic and allow for a rapid construction, as they act as a permanent formworks, but also increase the load carrying capacity. However, these tubes can still result in the failure of the column. The most common mode of failure within these tubes is through the steel yielding compressively, however failure can also occur through: crushing and cracking of concrete, as well as local buckling.

Concrete filled GFRP tubes are a new product that works in a similar manner to the previously mentioned steel tubes (Fam & Rizkalla 2015). The GFRP tube acts as a fixed formworks that serves as a noncorrosive flexure and shear reinforcement for concrete members. The GFRP shell provides confinement to the concrete, which in turn increases the strength and ductility. The GFRP tube also provided protection against extreme environmental effects. It is recommended that when GFRP tubes are used to externally confine concrete, that the concrete is also internally reinforced with steel bars. This is to overcome the brittle tensile failure of the tube (Yu & Teng 2011). Tensile failure of the GFRP tube is allowed as long as it occurs after the yielding of the steel reinforcement bars. Another common mode of failure is localised buckling.

2.4.2 Internal Confinement

Internal confinement uses the spacing of transverse reinforcement to increase the failure load and prevent crack control. By varying the design and spacing of the transverse reinforcement, the overall strength and behaviour of the concrete member. RC concrete can use steel or FRP reinforcement to internally improve the confinement.

At failure, tensions at the cover-core interface results in the spalling of the cover concrete (Foster, Kilpartick & Warner 2010). These tensions are caused by the confinement provided to the core. Once spalling of the cover concrete occurs, the core rapidly dilates and further increases in loads are possible, provided there is a balance between the loss of capacity of the section and an increase in strength due to the confinement.

Steel cages are the most common form of internally confining concrete compression members. Due to a high tensile strength, steel works very well with concrete, which cannot support tensile loads. The design of RC is such so that the core, which surrounded by the reinforcement cage, carries the majority of the applied loading, while the cover is provided to protect the bars from external conditions (Mander, Priestley & Park 1988). Steel reinforcement is set up in two directions, longitudinal and transverse. The longitudinal reinforcement helps carry the applied load, while the transverse reinforcement improves the confinement of the column. The spacing of these transverse reinforcement, the design of transverse reinforcement, as well as the volumetric ratio can all improve the axial capacity of the concrete member. A shorter spacing between the transverse reinforcement improves the concrete confinement as there is less room for the longitudinal bars to buckle as well as allowing for more transverse reinforcement to be present and carry more of the loading, which reduces the chance of concrete spalling of the core. The design of transverse reinforcement can also improve the confining effect. A continuous spiral will allow for a greater increase of strength compared to circular or rectangular ties. An increase of the volumetric ratio of transverse to longitudinal reinforcement will also allow for an increase in the axial capacity of the column. The effect of confinement is important as concrete begins spalling at a strain of 0.002. Once this strain is reached, the cover concrete will spall, however the core will continue to carry the load as long as it has been confined adequately. The benefits of confining concrete can be seen below in figure 2.6.

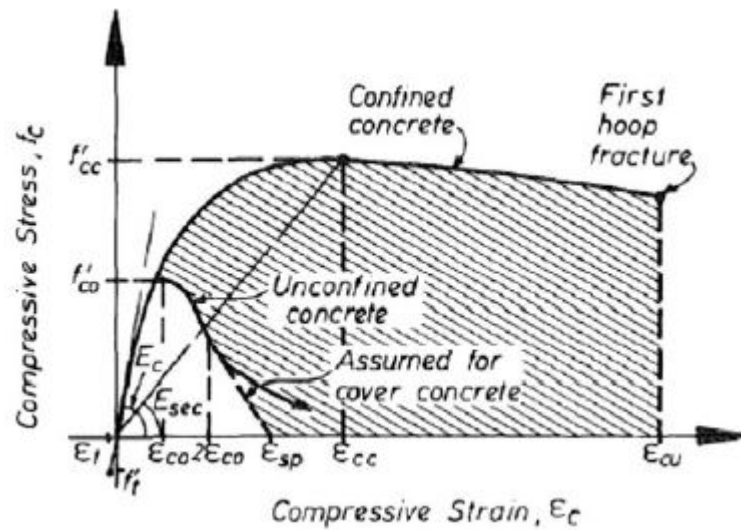


Figure 2.6: Theoretical stress-strain plot of confined concrete vs. unconfined concrete.

(Mander et al. 1988)

GFRP reinforcement has been found to be an effective method of confining concrete members in both flexure and shear. Due to this recommendation, the amount of literature is limited, however, despite numerous standards encouraging that GFRP is not used within compressive members, some papers (Ross 2007) believe that the use of FRP as reinforcement is essential to providing adequate confinement to columns. Ross states that GFRP reinforcement undergoes two types of loading while being subjected to compressive deformation. The GFRP has an axial loading applied, along with a transverse loading from the concrete core promptly expanding.

2.5 Factors Influencing the Axial Capacity

There are numerous factors that influence the axial capacity of concrete columns. These factors include: the longitudinal reinforcement ratio, the transverse reinforcement ratio, the overall dimensions of the column, the design of the transverse reinforcement, the effect of eccentricity along with numerous other factors. The sections presented have been determined as the most influential parameters that can affect the axial capacity of RC columns (Afifi 2013).

2.5.1 Longitudinal Reinforcement Ratio (ρ_{st})

The longitudinal reinforcement ratio is the ratio of the area of the bars to the total cross section of the column, and can be varied in two ways: increasing the size of the bars used, or inserting more longitudinal bars. There have been numerous studies into the effect of the longitudinal reinforcement ratio, such as the studies performed by Bjerkeli et al (1990), which looked at both increasing the number of bars along with the bar diameter. This studies used test columns that were 300 x 500 mm in size with a ranging compressive strength. To investigate the effect of an increase in bars, the study used specimens that were reinforced with 12 M16 bars along with 18 M16 bars. These specimens had a ρ_{st} of 1.59% and 2.38% respectively. This study concluded that the specimens with a higher reinforcement ratio sustained the ultimate load for a longer period of time, while the specimens with the lower reinforcement ratio deteriorated immediately after the peak load, as seen in figure 2.7.

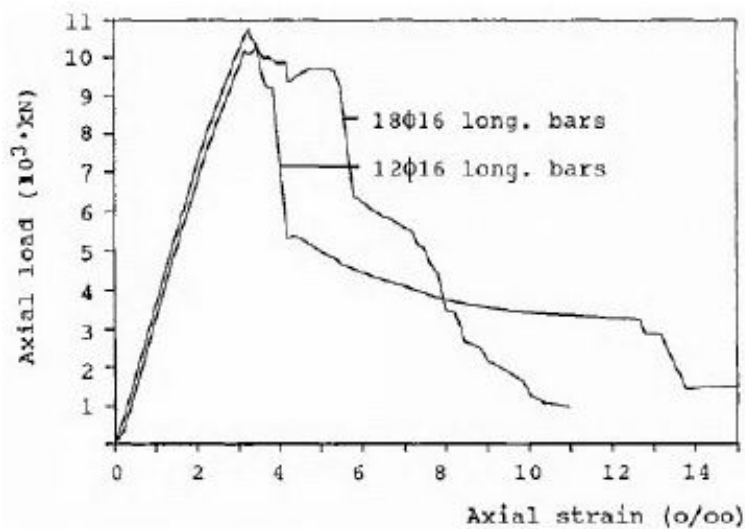


Figure 2.7: The effect of the longitudinal reinforcement on ductility

(Bjerkeli, Romaszewicz & Jensen 1990)

There have been many other studies into the effect of the longitudinal reinforcement ratio. Some of these studies have been performed by Xie (1997), and Lofty (2010). Xie looked into the effect of the reinforcement ratio on the moment around the centre line of the specimen, Lofty investigated the effect of the longitudinal reinforcement ratio on the axial behaviour of the column when using GFRP as longitudinal reinforcement.

Xies investigation was performed by testing three specimens with varied reinforcement ratios, being 1.3%, 1.96% and 3.26% (Xie, Elwi & MacGregor 1997). The testing program

of the test results indicated that an increase in the amount of longitudinal reinforcement will also result in an increase in the magnitude of the moment and axial loading that the column will be able to carry.

Loftys experimental program tested three different longitudinal reinforcement ratios, using specimens reinforced with 4 N12 bars, 6 N12bars and 8 N12 bars (Lotfy 2010). This study determined that increasing the ratio will also increase the ductility of the specimen, but also has an effect on the ultimate strain, the loading that cracking occurs, along with the ultimate load that the column resists. Lofty also stated that increasing the ratio from 0.723% (4 bars) to 1.08% (6 bars) had more of an effect on the behaviour than increasing from 6 bars to 8 bars.

2.5.2 Horizontal Reinforcement Ratio (ρ_s)

The horizontal reinforcement ratio is the ratio of transverse reinforcement to the total sectional view of the specimen. Similarly to the longitudinal reinforcement ratio, the horizontal reinforcement ratio can be increased by including more transverse reinforcement or increasing the size of the transverse reinforcement. The previously mentioned study performed by Sheikh and Toklucu also investigated the effect of the transverse reinforcement ratio on the behaviour of the column. To investigate this effect, a total of 27 specimens were prepared that were reinforced in the transverse direction by either spirals or hoop stirrups (Sheikh & Tokluc 1993). It was reported that the results showed that as the amount of transverse reinforcement was increased, the strength and ductility of the specimen was also increased.

Another study performed by Leung and Burgoyne investigated the effect of adding more reinforcement by varying the space or pitch of spiral reinforcement. This study used specimens that were 100 mm in height, with a pitch of the reinforcement of 10, 20, 30 and 50 mm (Leung & Burgoyne 2001). This test stated that as the pitch of the spiral was decreased, the peak load was increased.

De Luca also performed an investigation on the behaviour of columns reinforced transversely with GFRP hoop stirrups. The setup of specimens can be seen in figure 2.8, below (Luca, Matta & Nanni 2010). The results of this study showed that the GFRP reinforcement contributed approximately 5% of the total peak load, however, the small spacing

between hoop ties did not increase the peak capacity. It was noticed however that the spacing of the hoop ties did strongly contribute to the mode of failure of the specimen.

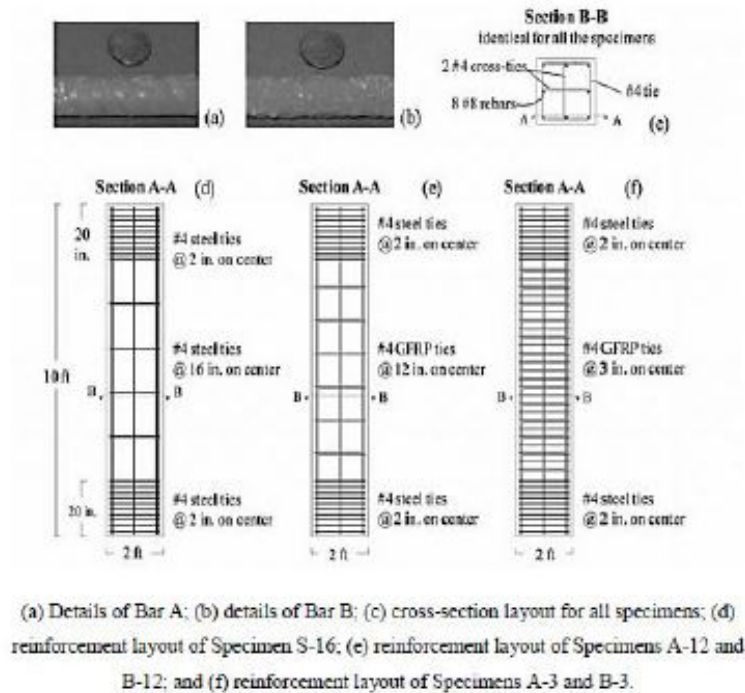


Figure 2.8: Reinforcement details for specimens.

(Luca et al. 2010)

2.5.3 Column Dimensions

The dimensions of the cross section also effects the axial capacity of a column. All dimensions (b, D and L) will affect the axial capacity. Sheikh and Tokluca investigated what effect the column diameter on the overall behaviour of the column (Sheikh & Toklcuc 1993). To maintain uniformity and maintain accuracy of results, all other variables were kept the same. It was discovered that the ductility of the specimen was significantly reduced as the diameter of the column was increased. Pessiki conducted a similar testing program (Pessiki, Graybeal & Mudlock 2001), however also varied the height of the specimens. Heights of 1420 mm and 2440 mm were tested, with the results showing that there was a higher strength of the concrete core and a higher obtained stress using a smaller height, due to the effect of the slenderness ratio.

Table 2.5: Summary of column tests.

(Tikka 2008)

Column	h	b	f_c	e/h	l/h	P_{test}	M_{test}	P_{comp}	M_{comp}	Strength Ratio
GFRP Reinforced										
A1	150	150	37.7	0.1	12	599	8.99	473	7.1	1.266
A2	150	150	37.7	0.23	12	381	13.34	323	10.8	1.180
A3	150	150	37.7	0.67	12	116	11.6	128	12.8	0.906
A4	150	150	45.8	∞	12	-	17.94	-	15.3	1.173
B1	150	150	37.7	0.1	12	563	8.45	469	7.0	1.2
B2	150	150	37.7	0.23	12	351	12.29	304	10.6	1.155
B3	150	150	37.7	0.67	12	119	11.9	131	13.2	0.908
C1	100	150	45.8	0.1	18	340	3.40	240	2.2	1.417
C2	100	150	37.7	0.23	18	188	4.32	143	3.3	1.316
C3	100	150	37.7	0.67	18	68	4.52	76	5.1	0.895
Steel Reinforced										
S1	150	150	45.8	0.23	12	601	21.04	460	16.1	1.307
S2	100	150	37.7	0.23	18	263	6.06	229	4.6	1.148

Tikka concluded that when an eccentric load is applied, longitudinal GFRP bars make a limited contribution to increasing the axial capacity.

2.5.5 Concrete Strength

The compressive strength of the concrete will also affect the axial capacity of the column. One popular investigation into the effect of the strength of the concrete on the axial capacity is the study performed by Razvi and Saatcioglu. In this study, twenty two columns were tested, with the concrete strength varied from 60 to 124 MPa (Razvi & Saatcioglu 1999). The results of this experiment stated that the concrete with a strength of 60 MPa obtained a higher ratio of strength development than the other specimens, which can be seen in figure 2.10. It was also noticed that as the strength was increased, there was a coinciding decrease in the deformation of each specimen.

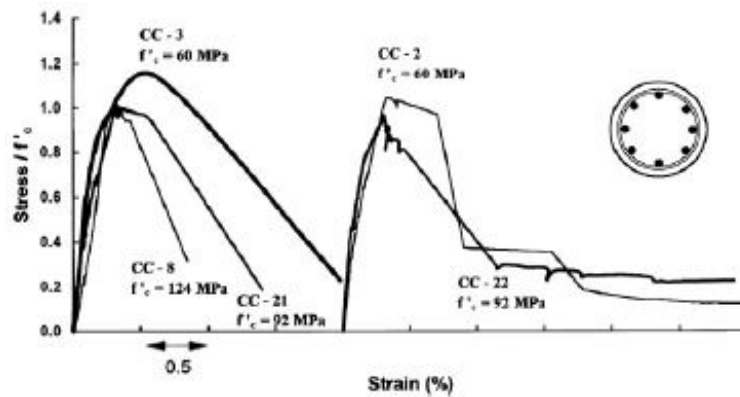


Figure 2.10: Effect of concrete strength on the axial capacity of confined concrete.

(Razvi & Saatcioglu 1999)

2.5.6 Transverse Reinforcement Yield Strength

The yield strength of a material is defined as the stress at which permanent deformation occurs (Edge 2015). There have been numerous studies into the effect of the yield strength of the transverse reinforcement on the overall behaviour of the column. One such study was conducted by Bing. This experiment used two types of steel transverse reinforcement, one with a yield strength of 445 MPa and the other with a ultra-high strength of 1315 MPa (Bing, Park & Tanaka 2001). The results of this experiment indicated that as the yield strength of the transverse reinforcement increases, the effect of confinement is increased, and in turn, the ultimate capacity is increased.

Likewise, when GFRP is used as transverse reinforcement, hoops or spirals that have a larger strength will allow for a larger ultimate load to be applied throughout the specimen (Afifi 2013).

2.6 Theoretical Modelling GFRP Reinforced Geopolymer Concrete

The standard practice when performing a theoretical analysis it to design the specimen as per the relevant standards and codes. There are multiple standards that relate to the design of concrete structures. In Australia, AS 3600-2009 is the most current code. However this code does not cover the use of FRP reinforcement or geopolymer concrete. Therefore existing equations from available literature are to be used. Four equations were

identified as suitable for use as a method of predicting the expected behaviour of FRP reinforced concrete. These equations were:

$$P_o = \alpha_1 * f_c * (A_g - A_f) \quad (2.3)$$

$$P_o = 0.85 * f_c * (A_g - A_f) \quad (2.4)$$

$$P_o = 0.85 * f_c * (A_g - A_f) + \alpha_g * f_{fu} * A_f \quad (2.5)$$

$$P_o = 0.85 * f_c * (A_g - A_f) + \epsilon_{f-peak1-ave} * E_f * A_f \quad (2.6)$$

Where:

- $\alpha_1 = 0.85 - 0.0015 * f_c > 0.67 = 0.79342$
- f_c =specified compressive strength of concrete=37.72 MPa
- A_g =gross section of concrete=49087.39 mm^2
- A_f =area of FRP tension reinforcement=1191.339 mm^2
- α_1 =reduction factor of GFRP bars compressive strength=0.35
- f_{fu} =ultimate tensile strength of FRP reinforcement=1184 MPa
- $\epsilon_{f-peak1-ave}$ =strain at initial peak loading=0.002
- E_f =modulus of elasticity of FRP reinforcement=62.9 GPa

These equations have been taken from the work of Axial Capacity of Circular Concrete Columns Reinforced with GFRP Bars and Spirals by Afifi, Mohamed and Benmokrane (Afifi, Mohamed & Benmokrane 2014) as well as Performance Evaluation of Concrete Columns Reinforced Longitudinally with FRP Bars and Confined with FRP Hoops and Spirals under Axial Load by Mohamed, Afifi and Benmokrane (Mohamed, Afifi & Benmokrane 2014).

2.7 Summary

It can be seen that this chapter investigated the behaviour of geopolymer concrete, GFRP material, the effect of confinement, factors influencing axial capacity as well as effective methods of creating a theoretical model of GFRP reinforced geopolymer concrete columns. It should be noted that of the studies investigated, most of them investigate the behaviour of geopolymer concrete with steel reinforcement or GFRP reinforced concrete made from Ordinary Portland cement. As previously stated, this significant gap in literature is the key reason behind this investigation into the behaviour of GFRP reinforced geopolymer concrete. It can be seen that geopolymer concrete results in a considerable decrease in carbon dioxide emissions, a stronger resistance to fire and chemicals, a higher early strength development, as well as a higher strength when compared to the properties of Ordinary Portland cement concrete. It was found that the advantages of GFRP reinforcement over steel reinforcement is that GFRP: is non-corrosive and therefore can be used in harsh environmental conditions, has a high tensile strength, as well as being lightweight and durable for transport. It was found that there is two methods used with GFRP confinement. These methods are external and internal confinement. External confinement involves wrapping the specimen in a GFRP wrap as a way of preventing spalling of the concrete core, while internal confinement is the more traditional method of confinement using bars and transverse ties to protect the core. It was also found that there are numerous factors that can affect the axial capacity of a column. These factors include, but are not limited to, the longitudinal reinforcement ratio, the horizontal reinforcement ratio, the column dimensions, the presence of eccentric loading, concrete strength as well as the yield strength of the transverse reinforcement. The presence of more longitudinal bars, will allow for a higher axial capacity along with larger axial strain resistance. A close spacing between transverse ties, was found to increase the strength and ductility of the column. Existing literature has found that the ductility of a circular column is reduced as the diameter of the column is increased. Literature has also found that if the height of a column is increased, so that the column is classed as slender, there will be a reduction in the strength of the column. It was found that eccentric loads result in a larger stress concentration on one side of the specimen. Studies have found that specimens that have a lower strength tend to result in a higher strength development ratio as well as a higher deformation when compared to concrete of a higher strength. It has been found by existing literature that as the yield strength of the transverse reinforcement is increased,

the effect of confinement is also increase, and in turn, the axial capacity of the column is increased. The creation of a theoretical model of an experiment is important as it allows for an approximation of the expected results that are to be obtained. It was found that there are four equations within existing literature that have been derived to calculate the capacity of concrete columns reinforced with GFRP. These equations will be used in the theoretical analysis for this research, with modifications made to allow for the geopolymer concrete.

Chapter 3

Materials and Methodology

3.1 Introduction

This chapter will discuss the research objectives, instrumentation used, the final test set up for the experimental testing as well as discussing the method of the analytical research program. As demonstrated from the review of current literature, more knowledge about the compressive behaviour of geopolymer concrete members that are internally reinforced with GFRP.

The research investigation was created to test the behaviour of circular geopolymer concrete columns internally reinforced with GFRP longitudinal bars and spiral or circular stirrups. Therefore analysis of the specimens will be done through both experimental testing as well as through a theoretical study using AS3600-2009, while making recommending changes to the existing equations to accommodate for the use of geopolymer concrete and GFRP reinforcement.

3.2 Material Properties

3.2.1 Geopolymer Concrete

Geopolymer concrete contains a geopolymer binder that is made from the chemical activation of two fly ash and blast furnace slag, instead of Portland cement (Wagners 2012).

This environmentally friendly binder has a lower embodied energy as well as reducing the amount of CO_2 by 60-70 %. Geopolymer concrete is available in a large variety of strengths ranging from 25 MPa right through to 50 MPa. The properties of the geopolymer concrete are shown below in table 3.1.

Table 3.1: Tested Properties of geopolymer concrete used.

Specimen Parameters	Tested Properties
Characteristic Compressive Strength at 28 days	37.72 MPa
Average Flexural Tensile Strength at 28 days	3.68 MPa
Average Modulus at 28 days	33 GPa

3.2.2 GFRP Reinforcement

GFRP is characterised by a high ultimate strain and low tensile elastic modulus. All GFRP reinforcement was manufactured by pultruding E-glass fibres impregnated with modified vinyl-ester resin and had a sand-coated surface to enhance the bond and force transfer between the GFRP reinforcement and the geopolymer concrete. Size 5 GFRP bars (figure 3.1) were used as longitudinal reinforcement was used along with sand coated GFRP spirals or circular ties (see figure 3.2 below) were used to reinforce the transverse direction. Table 3.2, below, shows the properties of a variety of GFRP bars. The properties of the spiral and hoop ties can be obtained from table 3.2 as the properties are the same as a size 3 bar. When the bars were tested using a Burn-out test, in accordance with ISO 1172:1996 (E) it was determined that the fibre content of the bars was 84.05%.



Figure 3.1: GFRP bars.



Figure 3.2: The spiral and circular ties used as transverse reinforcement.

Table 3.2: Mechanical properties of GFRP reinforcement.

(Maranan et al. 2015)

Bar Size	3	4	5	6
Diameter (mm)	9.5	12.7	15.9	19.0
Area (mm^2)	71.3	127	199	284
Modulus of Elasticity (GPa)	65.1 ± 2.5	65.6 ± 2.5	62.6 ± 2.5	63.7 ± 2.5
Tensile Strength (MPa)	1,372	1,312	1,184	1,105
Ultimate Elongation (%)	2.11	2.00	1.89	1.71

3.3 Specimen Details

As previously mentioned, six (6) specimens with changing parameters of: height, transverse reinforcement design and spacing of transverse reinforcement, with the details of each specimen shown in table 3.3 below. Each specimen was 250mm in diameter, with

twenty five (25) mm cover of concrete provided to the reinforcement cage, which had a diameter of 200mm. A schematic of the top view of the cages is provided below in figure 3.3.

Table 3.3: Specimen Details

Specimen Name	Transverse Reinforcement Type	Spacing (mm)
C1-0	None	-
C1-50	Hoop	50
C1-100	Hoop	100
C1-200	Hoop	200
S1-50	Spiral	50
S1-100	Spiral	100

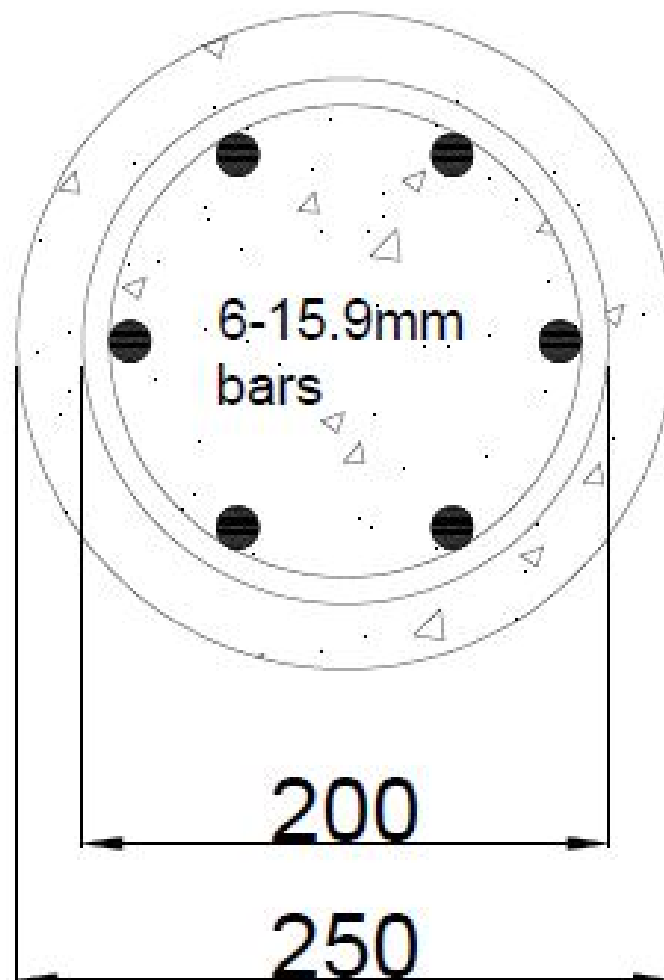


Figure 3.3: The top view of all specimens.

The spacing and type of lateral reinforcement as well as the height of the specimen were then varied to create six (6) different specimens. These specimens were designed in accordance with figures 3.4-3.5 below.

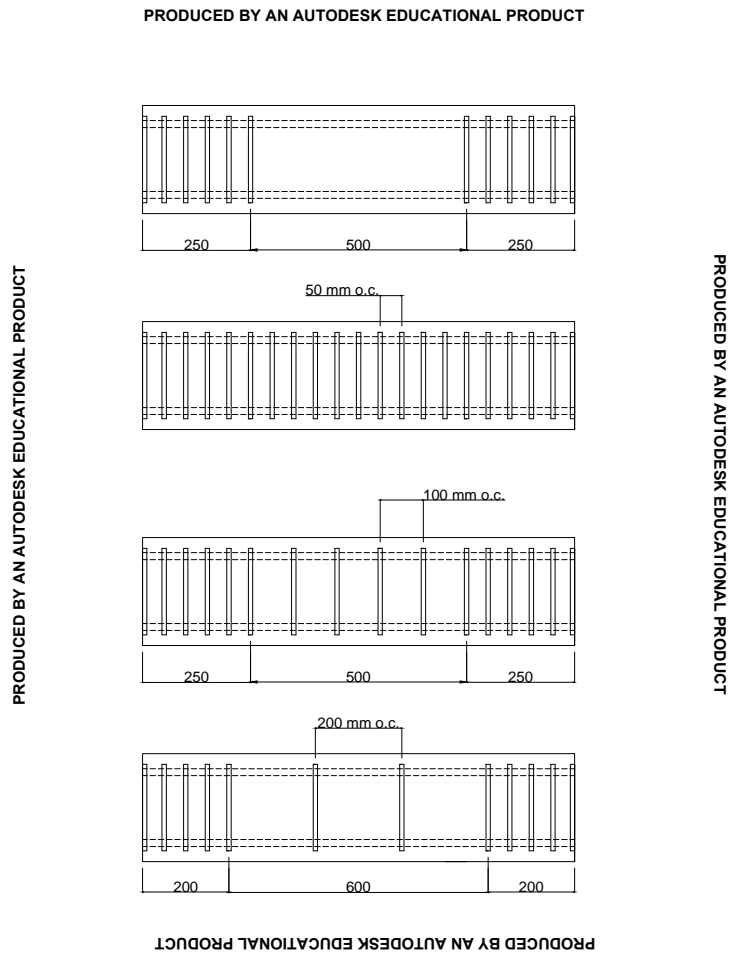


Figure 3.4: The design of the 1m specimens reinforced by circular ties.

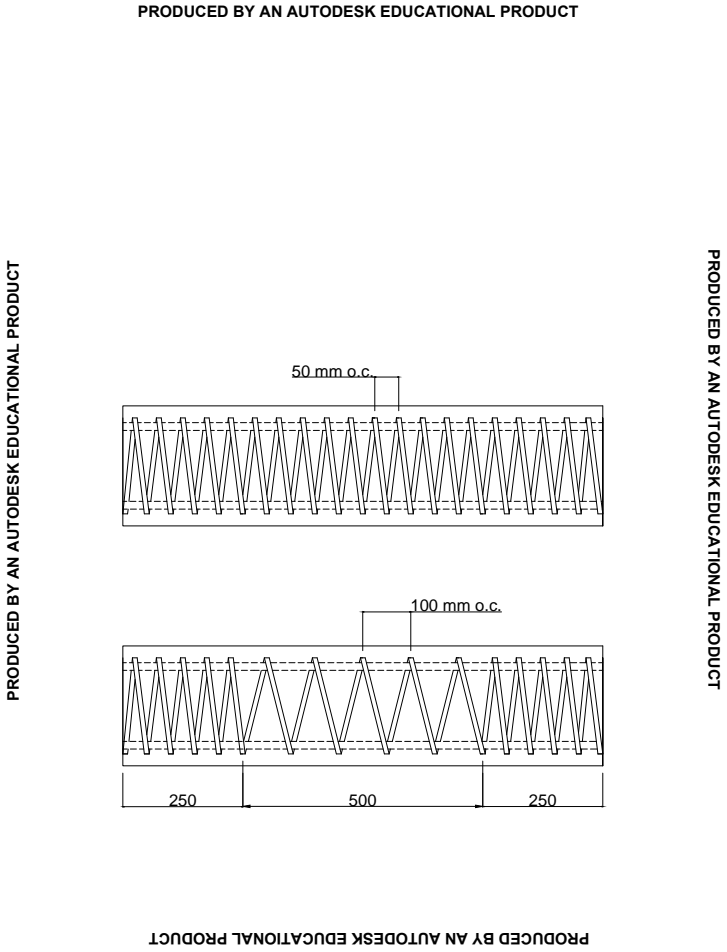


Figure 3.5: The design of the 1m specimens restrained by a continuous spiral.

3.4 Specimen Preparation

The GFRP reinforcement cages were constructed, in accordance with the plans shown above, using cable ties to attach the transverse reinforcement to longitudinal bars. After all eight cages were constructed, seen below in figure 3.6, a total of seven strain gauges were attached to the longitudinal bars, as well as transverse reinforcement.



Figure 3.6: The constructed reinforcement cages.

To do this, the reinforcement was sanded back to a smooth surface, before being covered with tape to prevent the gauge being damaged by the water within the concrete mix, seen below in figure 3.7.



Figure 3.7: The attachment of the internal strain gauges.

The 25mm spacers, figure 3.8, were then installed before inserting the cage into the formworks, figure 3.9. A steel bar was then inserted in each specimen, figure 3.10, to allow transportation via an overhead crane. The formworks was then placed into the frameworks before casting the concrete, figure 3.11.



Figure 3.8: The concrete spacers.



Figure 3.9: The formworks used for casting the specimens.



Figure 3.10: The internal configuration of each specimen.



Figure 3.11: The casting of the concrete.

After seven (7) days, the concrete specimens were removed from the formworks and left to continue the curing process. After leaving the specimens a total twenty eight (28) days, testing was performed on all specimens.

3.5 Instrumentation & Test Setup

To test the specimens several pieces of equipment were used. Photos of these items are included in Appendix C. These items included:

- 1x Hydraulic Jack
- 1x Circular Steel Plate $\phi 285\text{mm}$
- 4x Steel Bands
- 2x Neoprene Rubber 300x300x3mm
- 2x Neoprene Rubber 800x300x3mm
- 1x Square Steel Plate
- 1x Load Cell
- 1x Rectangular Steel Plate

- 1x Stringpot
- 2x Lasers
- 1x Square Steel Block
- 1x Aviary Wire 1400x900mm
- 1x Data Logger
- 1x Video Camera

The overall test setup for all specimens is shown in figure 3.12 below.

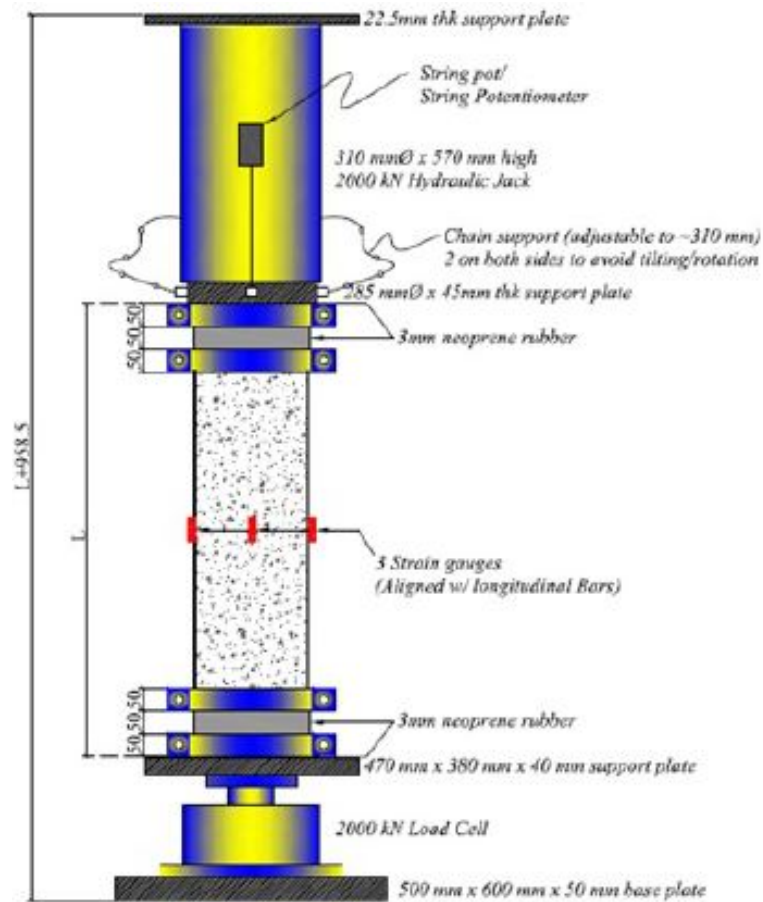


Figure 3.12: The setup of the instrumentation and specimen for testing

The orientation of each specimen, with reference to internal strain gauges and lasers is shown below in figure 3.13.

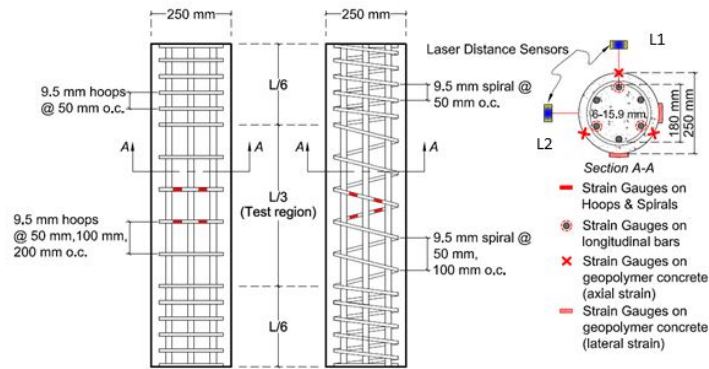


Figure 3.13: The setup of each specimen.

As seen from figures 3.12 and 3.13, the hydraulic jack was used to apply the compressive loading to the specimen, while the load cell was used to measure the loading that was applied. The circular steel plate was used to apply the loading from the jack over the entire column face. This was used due to the jack having a diameter of the face applying the load of 200mm, while the specimens were 250mm in diameter. The steel bands were used to ensure that the failure of the specimen was in the midsection, rather than in the areas where the confinement was uniform throughout the specimens. Neoprene rubber was placed between the specimens and the circular plate, as well as the square steel plate to ensure that there was a smooth even loading being applied to the specimen at all times. Neoprene rubber was also used between the steel bands and the specimens to prevent the bands damaging the concrete cover of the specimens. The square steel plate was placed on top of the load cell to provide a smooth surface that would cover the entire base of the specimen, similar to the circular steel plate. The rectangular steel plate was used as a base for the entire testing rig, to ensure that all testing equipment was set up straight and on a smooth surface. The stringpot and lasers were used to measure deformation. The stringpot measured the overall compressive deformation, while the lasers recorded the expansion of the mid span. The square steel block was used as a spacer, in case the hydraulic jack was raised up higher than needed. The aviary wire was used to protect testing equipment from flying debris, from the failure of the specimens. The data logger was used to list all data that was recorded by the strain gauges, stringpot, lasers and load cell. The video camera was used to record the testing of all specimens for later analysis.

3.6 Summary

It was determined that six specimens would be prepared of varying spacing between transverse reinforcement, along with type of transverse reinforcement. The specimens that were prepared consisted of a combination of 32MPa geopolymer concrete and GFRP reinforcement of size 5 for the longitudinal bars and size 3 for the transverse ties. The reinforcement cages were constructed as per the provided plans. Three strain gauges were attached to the longitudinal bars of each specimen, with four strain gauges being attached to the transverse ties. Once the gauges were attached to the specimens, the cages were inserted to the formworks, with concrete spacers of 32MPa used to provide adequate cover. The concrete was then cast, with the specimens removed from the formworks after a period of 7 days and tested after 28 days.

Chapter 4

Results and Observations

4.1 Introduction

This chapter of the dissertation will present all obtained results, including mode of failure of the specimens, as well as obtained strains from each of the twelve (12) strain gauges and the compressive deformation. This chapter will also state any observations made throughout the testing period. Assuming that concentric loading is applied, as aimed for, the load vs. strain graphs will be the same for all strain gauge readings. If these readings are not the same, it is possible that buckling has occurred.

4.2 Load vs Deformation Behaviour

To analyse the deformation of the specimens, three recording instruments were used, a stringpot as well as two lasers. The stringpot was used to determine the overall compressive deformation of the specimens, while the two lasers were used to measure the expansion of the mid-span of each specimen. Figure 4.1, below, shows the compressive deflection of all the specimens. The expansion of the mid-section of the specimens will be analysed in chapter 5.

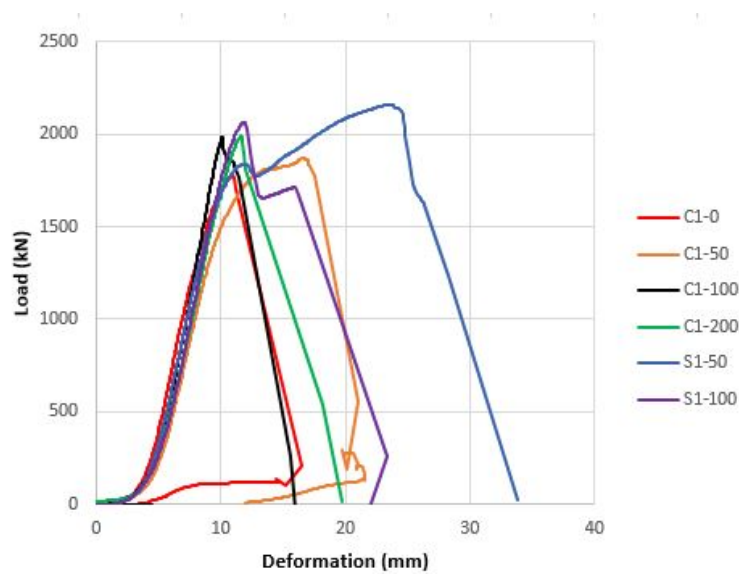


Figure 4.1: The deformation of all specimens.

It can be seen that all specimens had the cover concrete spall at a loading of approximately 1800kN. The peak loading reached by most specimens was 2000kN, with the exception of the S1-50 specimen, which reached a loading of approximately 2200kN. It can also be seen that this specimen also had the largest deformation out of all the specimens. This is because of the spiral reinforcement being a continuous piece of reinforcement and spreading strain throughout the entire specimen, rather than localising strain at a point.

4.3 Behaviour of the C1-0 Specimen

It was noticed that this specimen failed due to crushing of the core, as seen below in figure 4.2.



Figure 4.2: Core crushing failure of specimen C1-0.

The strain was also recorded on the longitudinal bars of the specimen, along with the external concrete face. These values were then plotted against the load, seen below in figures 4.3 and 4.4 below.

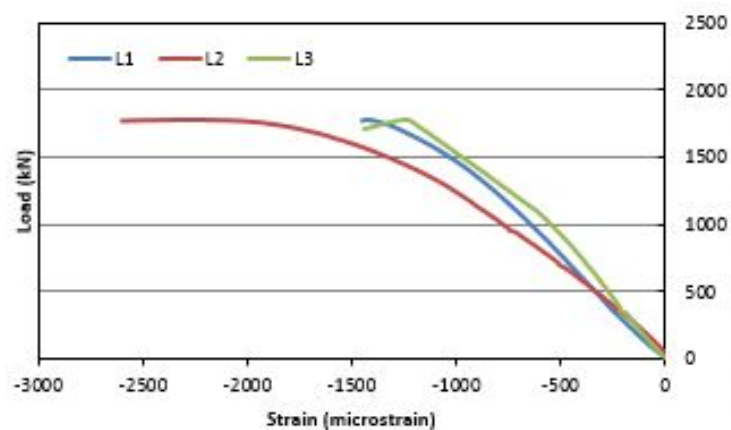


Figure 4.3: Load vs Longitudinal Strain for the C1-0 specimen.

It can be seen from figure 4.3 that all bars reached a maximum loading of approximately 1800kN. The bars labelled L1 and L3 reached a maximum of 1500 micro strain, while the bar labelled L2 recorded a strain of 2600 micro strain. There is many factors that could be the cause of this increase in strain on the L2 bar. These factors include: the effect of eccentricity, along with the non-conformity behaviour of concrete.

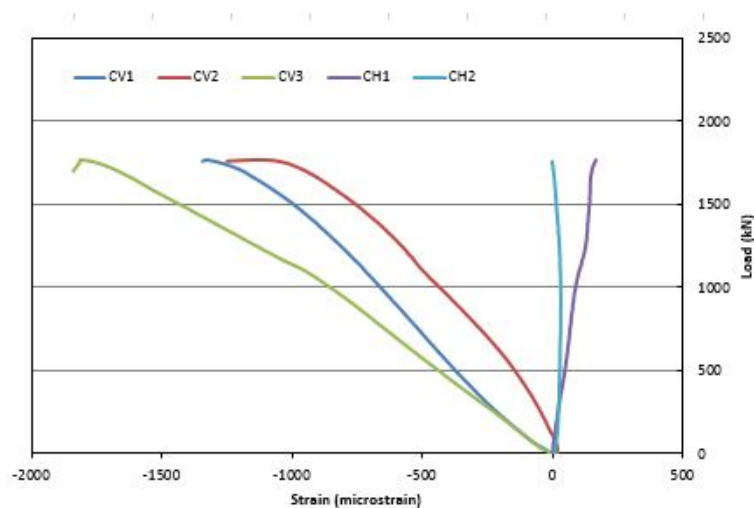


Figure 4.4: Load vs Concrete Strain for the C1-0 specimen.

For the external concrete strain, figure 4.4, it can be seen that the strain gauges marked CV1 and CV2 reached a strain of 1500 micro strain, while the strain gauge labelled CV3 reached a strain of 1800 micro strain. Similar to the internal longitudinal strain, this has been caused by the column being loaded eccentricity or due to concretes non-conforming nature. It can be seen that the strain in the transverse direction was uniform across the cross section of the specimen. Both transverse strain gauges, CH1 and CH2, reached a peak strain of approximately 250 micro strain, before the spalling of the concrete cover broke the gauges.

The recorded strain has also been compared to the observed behaviour of the specimen during testing. It was observed that there was no cracking of the specimen until the peak load was reached. This specimen was also the quickest to fail due to the lack of transverse reinforcement.

4.4 Behaviour of the C1-50 Specimen

The mode of failure of the C1-50 specimen was also core crushing, seen below in figure 4.5.

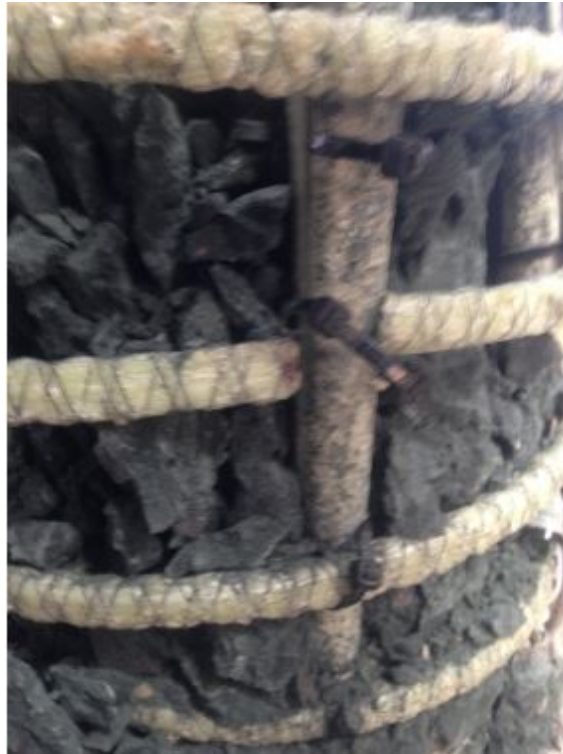


Figure 4.5: Core crushing failure of the C1-50 specimen.

The strain present in the longitudinal bars, circular ties at the midpoint of the specimen and external concrete surface was also recorded, show below (figures 4.6-4.8 respectively) plotted against the applied load.

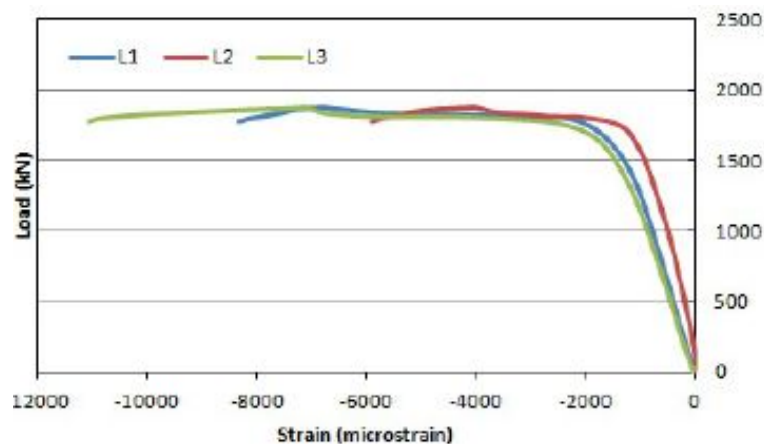


Figure 4.6: Load vs Longitudinal Strain for the C1-50 specimen.

It can be seen from figure 4.6 that all three bars behaved in a similar manner until a strain of 6000 micro strain. This point was where the L2 bar failed, while the L1 bar recorded over 8000 micro strain and the L3 bar recorded an excess of 11000 micro strain. This increase in recorded strain can again be put down to the column either being loaded off centre or due to the non-conforming nature of concrete as a material.

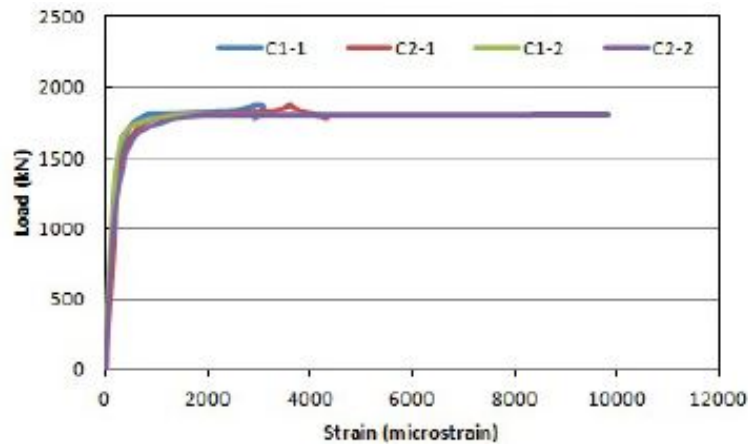


Figure 4.7: Load vs Transverse Strain for the C1-50 specimen.

It can be seen from figure 4.7 that all ties behaved in a similar manner, with the gauges labelled C1-1 and C2-1 failed at approximately 4000 micro strain. The other two strain gauges, C1-2 and C2-2, recorded a strain of approximately 10000 micro strain. This premature failure was due to C1-1 and C2-1 being located close to the lapped edge of the tie. As the tie expanded, the lapped length slowly decreased, which caused a false reading of the strain gauges in this location, due to there being less strain present in this area.

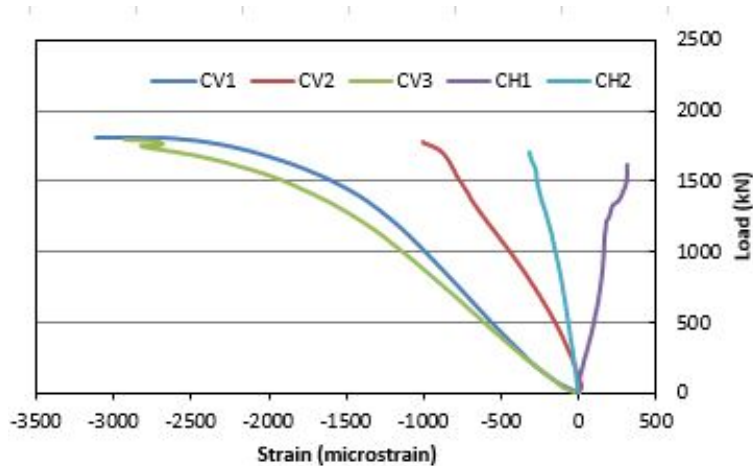


Figure 4.8: Load vs Concrete Strain for the C1-50 specimen.

It can be seen from figure 4.8, that the strain gauges labelled CV1 and CV3 behaved in a similar manner, both reaching a recorded strain of approximately 3500 micro strain before failing, while the strain gauge labelled CV2 had a lower strain recorded, approximately 1000. This can explained with the same reasoning that was used in the analysis of the longitudinal bars, that the specimen was loaded off centre and therefore eccentricity came into effect, or that the non-conforming nature of concrete has had an effect in the results. It can also be seen that both the strain gauges recording horizontal strain on

the concrete surface, CH1 and CH2, behaved in a similar manner, reaching a strain of approximately 5500 micro strain. This again can be explained by the specimen being loaded in eccentricity or that the nature of the concrete has played an effect in the testing of this specimen, however it is also possible that one of the strain gauges was placed over a small crack in the specimen, which would also explain why the two transverse strain readings were not identical. The recorded strain has also been compared to the observed behaviour of the specimen during testing. Once again, it was observed that there was no cracking of the specimen until the peak load was reached. After this, longitudinal cracks were observed on the specimen, until the ultimate load was reached and the core failed. It was also observed that splitting of the longitudinal bars, a protrusion of the longitudinal bars from the base, as well as cracking of the patched base also occurred within the testing of this specimen, shown below in figure 4.9-4.11 respectively.



Figure 4.9: Bending of the longitudinal bars.



Figure 4.10: Longitudinal bars extruding from the base.



Figure 4.11: Cracking of the patched area.

4.5 Behaviour of the C1-100 Specimen

It was observed that this specimen failed due to shear failure, seen below in figure 4.12.



Figure 4.12: Shear failure of the C1-100 specimen.

The internal longitudinal strain (figure 4.13), internal horizontal strain (figure 4.14) and external concrete strain (figure 4.15) was again recorded and plotted against the applied load and are all shown below.

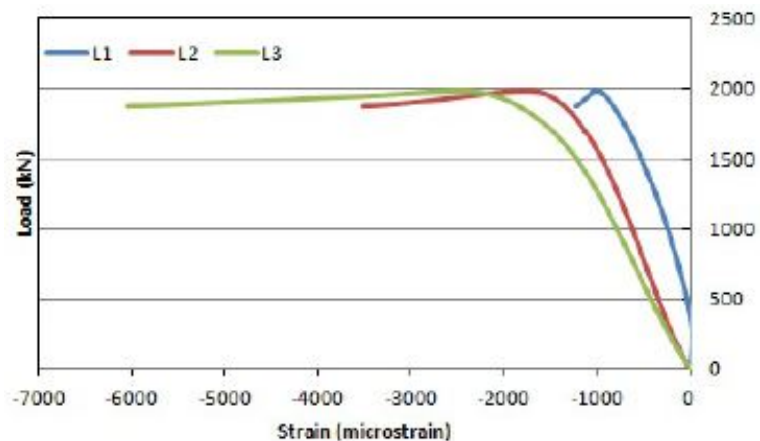


Figure 4.13: Load vs Longitudinal Strain for the C1-100 specimen.

It can be seen from figure 4.13, above, that the bars behaved in a similar manner, with the bar labelled L1 reaching a strain of approximately 1100 micro strain, the L2 bar reaching a strain of approximately 3800 micro strain and the L3 bar reached a strain of approximately 6000 micro strain. This figure suggests that this specimen has been loaded slightly off centre, closer to the L2 and L3 bars, which is why this specimen has a much

higher strain reading for these two bars.

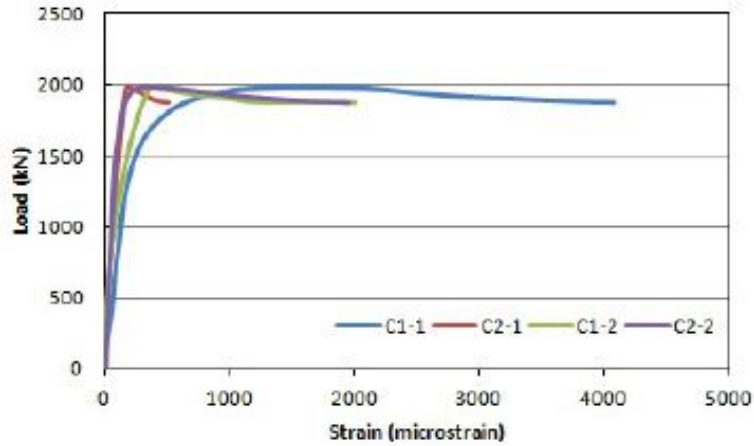


Figure 4.14: Load vs Transverse Strain for the C1-100 specimen.

It can be seen from figure 4.14 that the hoop ties labelled C1-2 and C2-2 behaved in the exact same manner, reaching a strain of approximately 2000 micro strain. The strain gauge labelled C1-1, doubled this reading, reaching a strain of approximately 4000 micro strain, while the strain gauge labelled C2-1 recorded a strain of approximately 500 micro strain. This was because of the way the specimen was constructed. The two strain gauges that recorded the same reading, C1-2 and C2-2, were located near the spliced length of the hoop ties, while the C1-1 tie was located between the L2 and L3 bars, which the loading was applied nearest to (figure 4.13), while the C2-1 bar was located near the L1 bar, which had a lower strain due to the off centre loading.

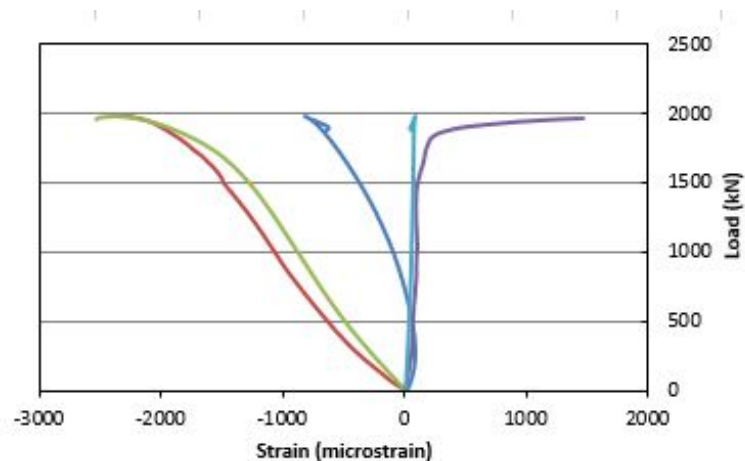


Figure 4.15: Load vs Concrete Strain for the C1-100 specimen.

It can be seen from figure 4.15, above, that the strain gauges labelled CV2 and CV3 behaved in a similar manner, reaching a maximum strain of approximately 2000 micro strain. The strain gauge labelled CV1 however recorded a reading of approximately half

this, 1000 micro strain. Once again, this low recorded strain for CV1, is due to effect of eccentricity. The strain gauges that were setup to record horizontal strain on the concrete surface also recorded readings that were different to each other. The strain gauge labelled CH1, recorded a reading of approximately 4500 micro strain, while the strain gauge labelled CH2 failed to record any reading. As all strain gauges were tested and found to be operational before the specimen was tested, it is possible that this strain gauge was located on a crack in the concrete surface, and therefore did not record any data. Once again, it was observed that there was no cracking of the specimen until the peak load was reached. After this, longitudinal cracks were observed on the specimen, until the ultimate load was reached and the core failed. Despite failing in a similar manner to the C1-50 specimen, the time taken for failure of the specimen to occur was quicker than the C1-50 specimen. Splitting of the longitudinal bars were again observed within testing this specimen, however splitting of the circular ties were also observed within this specimen, seen below in figure 4.16.



Figure 4.16: Splitting of the longitudinal bars and separation of circular ties for the C1-100 specimen.

4.6 Behaviour of the C1-200 Specimen

It was again observed that shear was responsible for the failure of the C1-200 specimen, as seen below in figure 4.17.

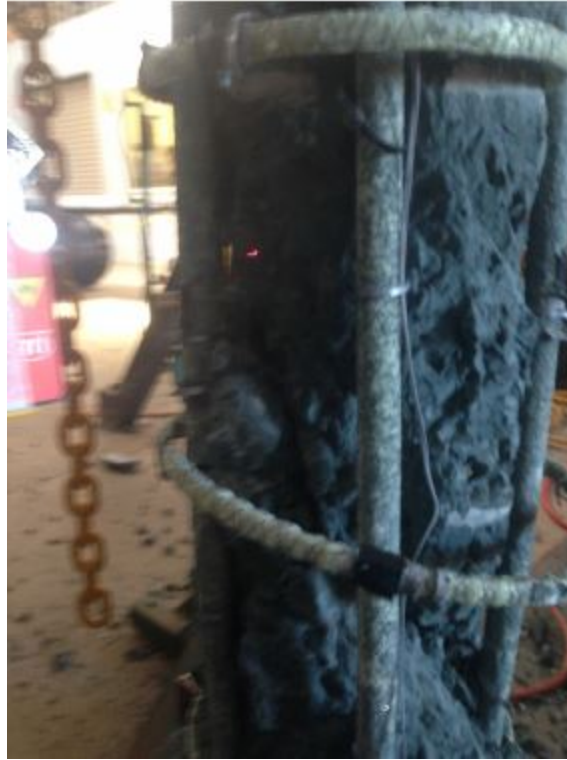


Figure 4.17: Shear failure of specimen C1-200.

The internal longitudinal strain, internal horizontal strain and external concrete strain are shown below in figures 4.18-4.20 respectively.

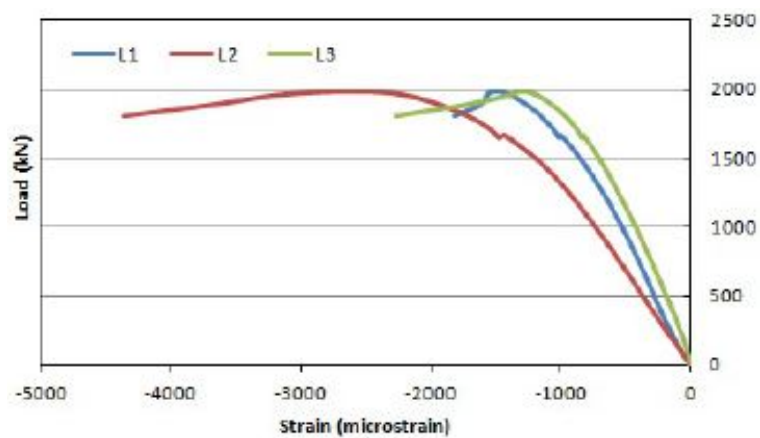


Figure 4.18: Load vs Longitudinal Strain for the C1-200 specimen.

It can be seen from figure 4.18 that the bars labelled L1 and L3 behaved in a similar manner, reaching a strain of approximately 2200 and 2000 micro strain respectively. The

strain gauge labelled L2 however recorded a strain of approximately 4500 micro strain. This was because of the effect of eccentricity, which was present due to the specimen being loaded closer to the L2 bar.

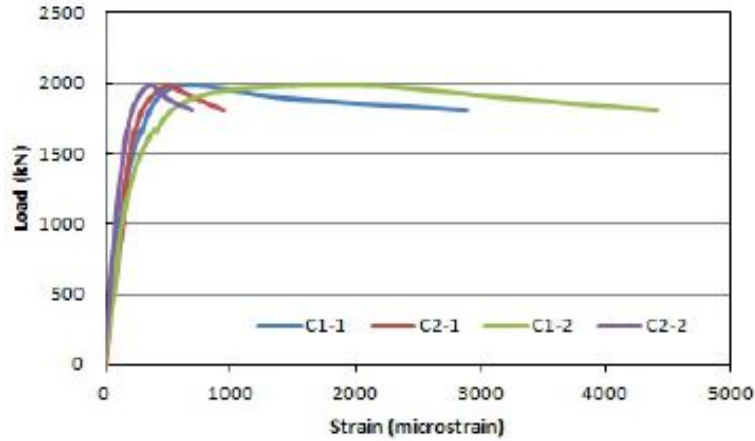


Figure 4.19: Load vs Transverse Strain for the C1-200 specimen.

Figure 4.19, above, shows the strain recorded in the transverse ties for the C1-200 specimen. It can be seen from this figure that two strain gauges, C2-1 and C2-2, reached a maximum strain of 1000 micro strain, while the strain gauge titled C1-1 reached a strain of the approximately 3000 micro strain, and the remaining strain gauge, C1-2, recorded a reading of approximately 4500 micro strain. The construction of the reinforcement cage for this specimen contributed to the recorded strain readings of this specimen. The C1-1 and C2-1 specimens were the two strain gauges that were located closest to the lapped edge of the hoop ties, however the hoop tie was orientated in such a way that the C1-1 strain gauge was located near the L2 bar, and therefore had a higher strain reading than other gauges that were on the continuous part of the ties.

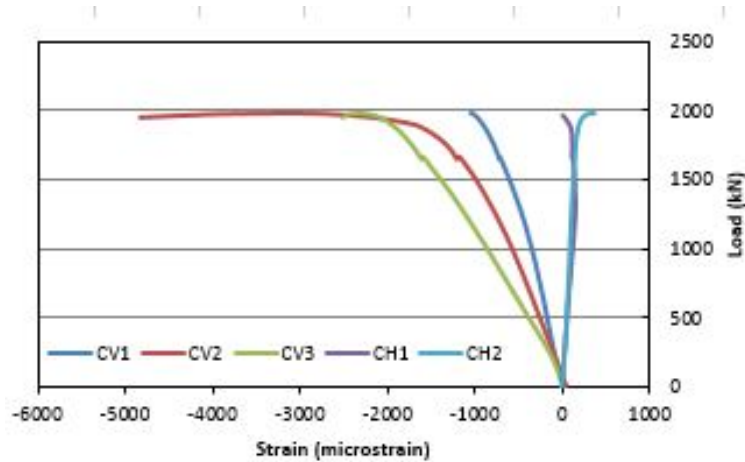


Figure 4.20: Load vs Concrete Strain for the C1-200 specimen.

The above figure, 4.20, shows the behaviour of the external concrete strain. It can be seen from this figure that the strain gauges CV2 and CV3 recorded a similar behaviour, recording approximate strains of 5000 micro strain and 3000 micro strain respectively. The strain gauge CV1 recorded a strain of approximately 1000 micro strain. As per the recorded strain readings for the longitudinal bars, it can be seen that the specimen was loaded closer to the L2 bar (CV2) than other longitudinal bars. The strain gauges designed to record horizontal strain, CH1 and CH2, also behaved in a similar manner while the load was being applied, however after reaching the maximum loading, the CH1 strain gauge recorded a decrease in strain, while the CH2 strain gauge recorded a minor increase in strain. This was again because of the location of the gauges, with the CH1 gauge being closest to the loading.

Similar to the previous specimens, it was observed that there was no cracking of the specimen until the peak load was reached. After this, the specimen behaved in a similar manner to the C1-0 specimen. This was due to the large spacing between the transverse ties, not allowing for sufficient confinement of the core.

4.7 Behaviour of the S1-50 Specimen

It was observed that the S1-50 specimen failed due to crushing of the core, which can be seen below in figure 4.21.



Figure 4.21: core crushing of the S1-50 specimen.

The internal longitudinal and horizontal strains along with the external concrete strain were again graphed against the applied load, shown below in figures 4.22-4.24 respectively.

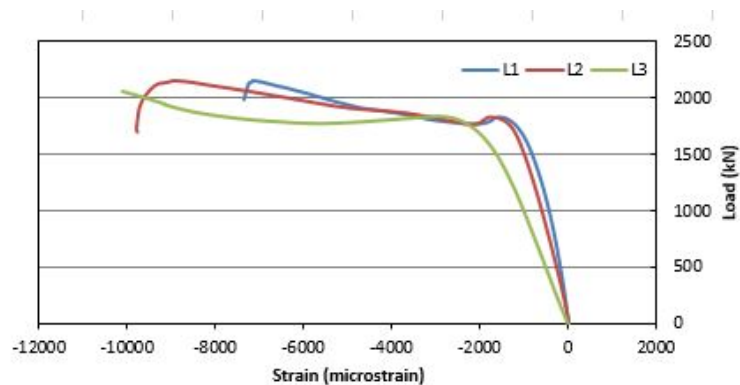


Figure 4.22: Load vs Longitudinal Strain for the S1-50 specimen.

It can be seen from figure 4.22, that the strain in all bars behaved in the same manner. All bars recorded two peak loads. The first peak loading, which is the peak load of the other specimens, is the loading at which the concrete cover spalled at. The second peak loading was the effect of the confinement of the core. It can be seen that the strain gauge of the longitudinal bar labelled L1 reached a peak strain of approximately 7000 micro strain. The strain gauge on the L2 bar recorded a peak strain of approximately 9000 micro strain, while the strain gauge that was located on the L3 bar recorded a peak

loading of approximately 10000 micro strain. These bars exhibited this uniform behaviour because of the design of the transverse ties. As the spiral tie was a continuous piece of reinforcement, the strain was easily distributed evenly throughout the whole specimen, and therefore prevented any localised strain being placed on the longitudinal bars.

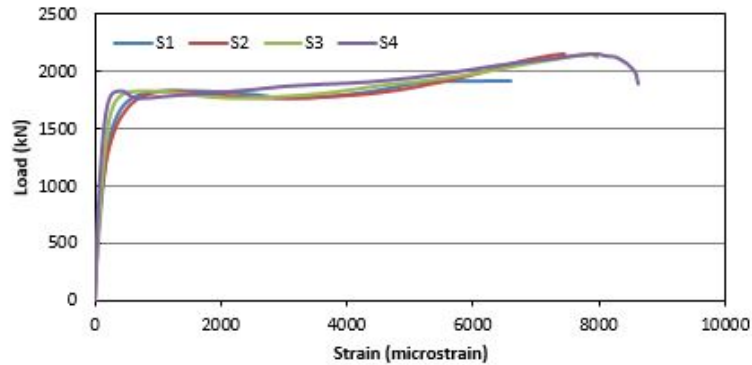


Figure 4.23: Load vs Transverse Strain for the S1-50 specimen.

Figure 4.23, seen above, shows that all strain gauges recorded a similar strain throughout the transverse reinforcement. It can be seen that the maximum strain recorded by the strain gauges was within the range of approximately 5000 micro strain (S1) to 8000 micro strain (S4). This closeness of the recorded values was because of the design of the transverse reinforcement. As this specimen was reinforced with a continuous spiral tie, the strain was distributed throughout the entire specimen, rather than localised in a particular area.

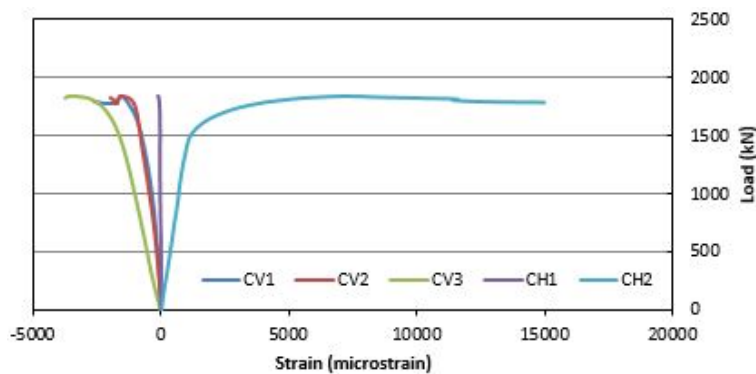


Figure 4.24: Load vs Concrete Strain for the S1-50 specimen.

Figure 4.24, above, shows the vertical and horizontal strain recorded on the external concrete surface of the specimen. It can be seen that the strain recorded in the direction of the longitudinal reinforcement, acted in a similar manner, reaching a peak strain of approximately 2500 micro strain, recorded by the strain gauge labelled CV3. The strain in the transverse direction did not however behave in a similar manner. The strain gauge

labelled CH1 recorded very little strain until the peak load was reached before reaching approximately 10000 micro strain after this point. This could be due to the strain gauge being located on a small crack in the concrete specimen, and therefore prevented the strain from being recorded until the crack was closed from the compressive behaviour of the specimen. The CH2 strain gauge however had a gradual increase in the strain and loading, before reaching a maximum strain of approximately 15000 micro strain. Similar to the previous specimens, it was observed that there was no cracking of the specimen until the peak load was reached. After the first peak loading occurred, it was observed that there were longitudinal cracks that ran down the entire specimen. The failure of this specimen was gradual due to the close spacing between the spiral tie providing more than efficient confinement to the core of the specimen. It was also observed that the longitudinal bars extended out of both ends of the specimen, as seen in figure 4.25.



Figure 4.25: The extrusion of longitudinal bars of the specimen S1-50 from the top of the specimen (left) as well as the base (right).

4.8 Behaviour of the S1-100 Specimen

The observed failure of the S1-100 bar was also through core crushing, as seen below in figure 4.26.



Figure 4.26: The core crushing of specimen S1-100.

The internal longitudinal strain, internal horizontal strain and external concrete strain are shown below in figures 4.27-4.29.

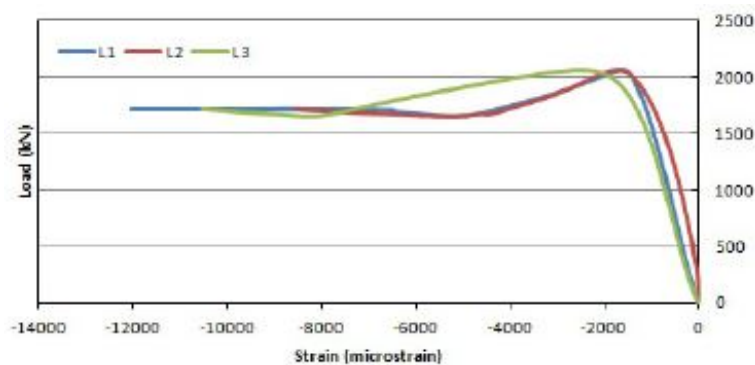


Figure 4.27: Load vs Longitudinal Strain for the S1-100 specimen.

It can be seen from figure 4.27, that the strain recorded in the longitudinal bars was fairly uniform across the three bars with strain gauges attached. These bars recorded

a strain of approximately 12000 micro strain. Similarly to the S1-50 specimen, this specimen exhibited this trend due to the type of transverse reinforcement. The continuity of the spiral tie allowed strain to be distributed over the entire specimen, which prevented localised strain and failure of the transverse ties.

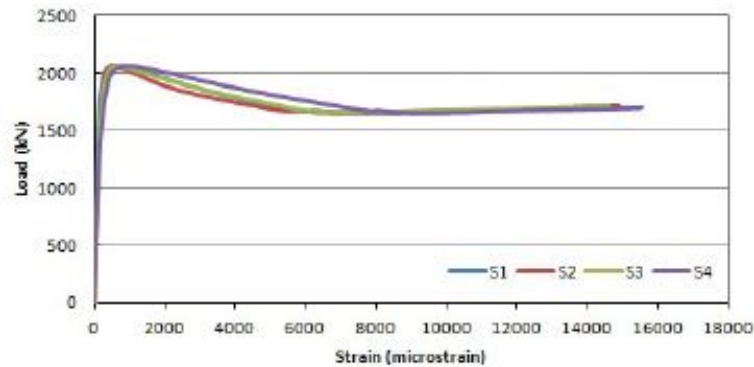


Figure 4.28: Load vs Transverse Strain for the S1-100 specimen.

Figure 4.28 shows that the strain on the spiral tie was also uniform across the specimen. It can be seen that the ties recorded a strain of approximately 16000 micro strain in all strain gauges. This uniformity is because of the spiral tie being one continuous piece of reinforcement, and therefore spreading the strain across the entire specimen, rather than localising strain in a particular area.

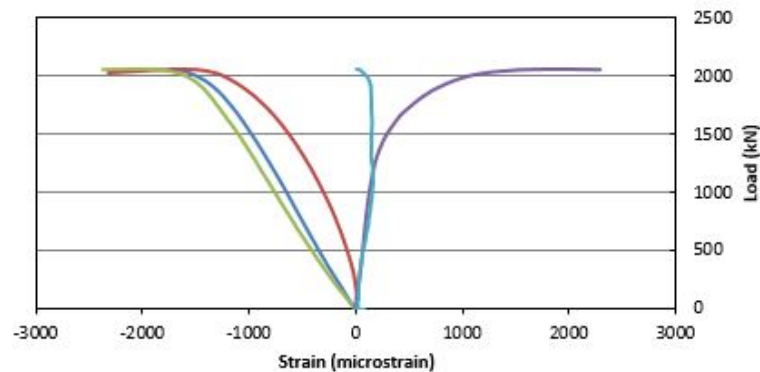


Figure 4.29: Load vs Concrete Strain for the S1-100 specimen.

It can be seen from figure 4.29 that the external concrete strain recorded in the direction of the longitudinal bars acted uniformly across the entire specimen. It can be seen that all three strain gauges recorded a maximum strain of approximately 2000 micro strain while the loading was being applied. The two strain gauges recording strain in the direction of the transverse ties also recorded strains that were similar to each other, until a loading of approximately 1500 kN. After this point, the strain recorded by the gauge CH1 rapidly increased, to approximately 3500 micro strain, while the strain recorded by CH2 hardly

increased, recording a peak strain of approximately 250 micro strain. As per the reading from the S1-50 specimen, this strain gauge could have been located on a small crack in the surface, and therefore limited the quality of the reading. Similar to the previous specimens, it was observed that there was no cracking of the specimen until the peak load was reached. After the first peak loading occurred, an immediate cracking of the concrete cover was observed. After this, the ultimate load was reached quicker than the S1-50 specimen, due to the greater spacing in the transverse direction, however, the failure did occur slower than the C1-100 specimen. Splitting and buckling of the longitudinal bars was also observed within this specimen, as seen in figures 4.30 and 4.31.



Figure 4.30: The buckling of the longitudinal bars.



Figure 4.31: The splitting of the vertical bars.

4.9 Conclusion

It can be seen that the maximum load applied to any of the specimens was approximately 2200kN. However, each specimen failed in its own unique way. It can also be seen after approximately 1800kN the load tends to plateau while the strain increases. Despite reading of the strain recorded by the gauges being slightly different, buckling of the specimens can be ruled out as this can be put down to the loading not being applied through the centre of each specimen.

Chapter 5

Discussion of Results and Effect of the Test Variable

5.1 Introduction

This chapter aims to discuss the obtained results, investigate the effect the three test variables on the overall behaviour of the specimens, along with providing a theoretical prediction of the observed strength. To do this, the three variables, being deflection of the specimens, spacing of transverse reinforcement and type of transverse reinforcement used, will be analysed separately. This study is significant as there is limited knowledge of the behaviour of GFRP in compression, as well as GFRP reinforcement having never before been tested with geopolymer concrete. There were limitations in this study however. These limitations were time constraints as well as limited resources. The limited resources only allowed for the construction of one of each of the specimens, so it is assumed that all results are correct. The theoretical analysis was performed through the use of equations from CSA S806-12 along with existing literature. As none of these sources account for the use of geopolymer concrete, there have been slight changes made to the analysis to more accurately match the observed results.

5.2 Effect of Spacing

The effect of spacing of transverse ties is an important parameter in the design of reinforced concrete columns. If the ties are spaced to far apart, the member may fail due to shear. Therefore the spacing of ties will not only have an effect on the ultimate load carried by the column, but also on the amount of strain that is carried in not only the transverse ties but the longitudinal bars as well. To properly analyse the effect of the spacing of ties, specimens will be separated into two groups, being those reinforced with hoop ties and those reinforced with a continuous spiral. Within these two groups, the strain that was carried by the longitudinal bars as well as the transverse bars will be analysed.

5.2.1 Spacing of Hoop Ties

Figures 5.1 and 5.2, below, show the average strain carried by the longitudinal and transverse bars, for specimens C1-0, C1-50, C1-100 and C1-200, respectively.

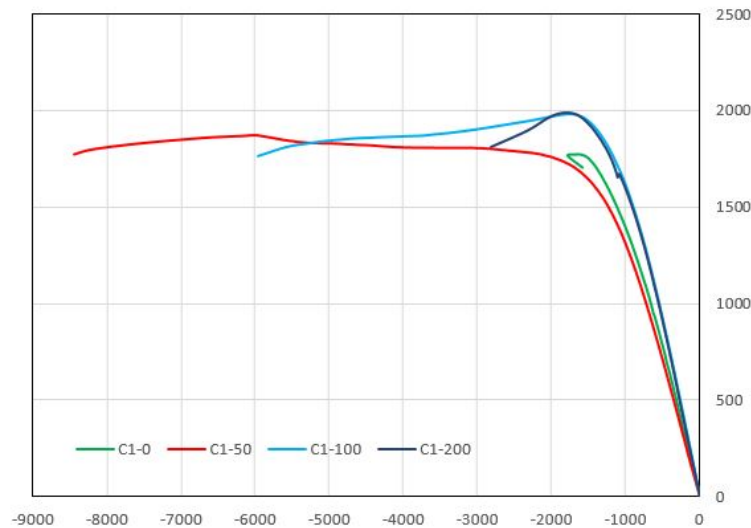


Figure 5.1: The average strain carried by the longitudinal bars transversely reinforced by hoop ties.

As seen in figure 5.1, above, the C1-0 specimen, behaved as expected, having the lowest resistance to the loading, as well as carrying the smallest amount of strain within the longitudinal bars. This is due to there being no transverse reinforcement to confine the concrete core after the cover concrete began spalling. It can be seen that when hoop ties were introduced, the load capacity was enhanced, with the new ultimate load being

approximately 2000kN. The ductility of the specimens were also increased, which can be seen by the increase of the strain that is carried by each specimen. It was observed that a reduction in the spacing between the ties resulted in a higher strain within the longitudinal bars. It was also observed that the C1-50 specimen had a peak loading that was less than the other specimens that were reinforced with hoop ties, which was not predicted. This was a result of the way this specimen was cast. As the hoop ties were close so closely spaced, the geopolymer concrete did not pass through the ties to create an effective cover despite meeting all vibratory requirements during casting.

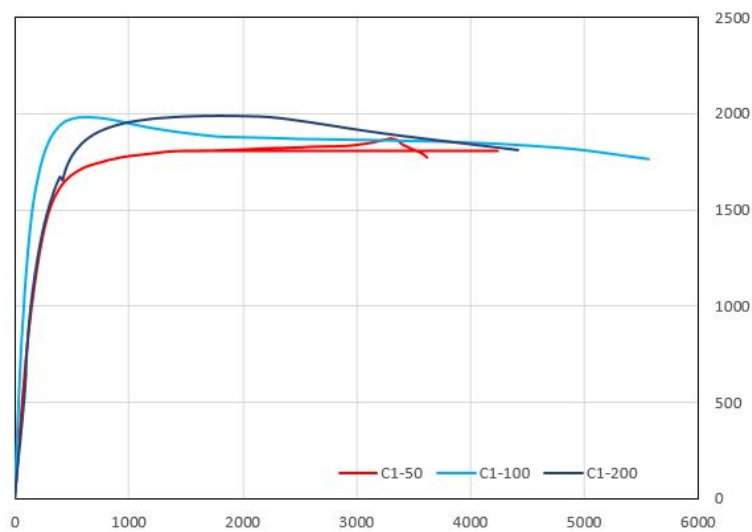


Figure 5.2: The average strain carried by the transverse hoop ties.

The C1-0 specimen has been excluded from figure 5.2, above, due to the specimen not having transverse reinforcement. It can be seen that as the spacing between the hoop ties was decreased, the amount of strain in the ties was increased. However, the C1-50 specimen had the lowest amount of transverse strain recorded. This is a result of the lapped join of the ties splitting apart under column expansion, as seen in the previous chapter. This concurs with findings by Sheikh and Tokluca along with De Luca. These findings stated that as the horizontal reinforcement ratio is decreased, the total amount of strain carried by the specimen, along with the ductility of the specimen would also decrease.

It can be seen from figures 5.1 and 5.2, both above, that there is a linear load-strain relationship until a loading of approximately 1800kN, which was when the spalling of the concrete cover occurred. After this, the loading slightly increases to approximately 2000kN before not changing while the strain is increased. This occurred due to the concrete core taking most of the loading.

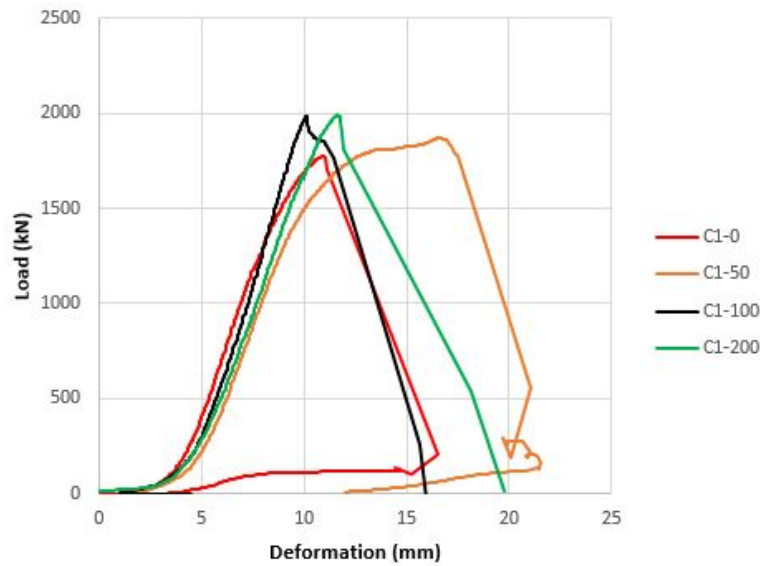


Figure 5.3: The compressive deflection of the specimens reinforced with hoop ties.

When the deflection of the specimens reinforced with hoop ties are analysed, figure 5.3 above, it can be seen that both the C1-0 specimen had the lowest peak loading of approximately 1800kN. In accordance to the literature, this specimen should have had a strength that was approximately 85% of the strength of the test cylinders that were prepared. When this ratio was calculated, it was found that the specimen had a strength of approximately 94% of the cylinders. This difference in predicted strength to observed strength can be put down to the presence of the longitudinal bars. When transverse hoop ties are added, the ductility and loading capacity of the specimens are increased. The C1-100 and C1-200 specimen had an ultimate loading of 2000kN. The result that was not was that of the C1-50 specimen. It was predicted that this specimen would have the highest ultimate load and deformation. It was determined that the reason behind the lower initial peak was due to the concrete not being able to pass between the small spacing between the ties. This was because of the large amount of transverse ties preventing continuity of the concrete within the specimen. In the C1-50 and C1-100 specimens a second peak is evident. This second peak can be calculated using the loading at the peak, along with the cross sectional area of the core, due to the cover concrete having spalled. The loading that this peak occurs at is dependent on how effectively the core of the specimen is confined. The deformation shown in the above graph is the compressive deflection. The mid-span expansion was also recorded, through the use of two lasers, placed at right angles to each other. The graph showing the mid-span expansion of the C1-0 specimen can be seen below.

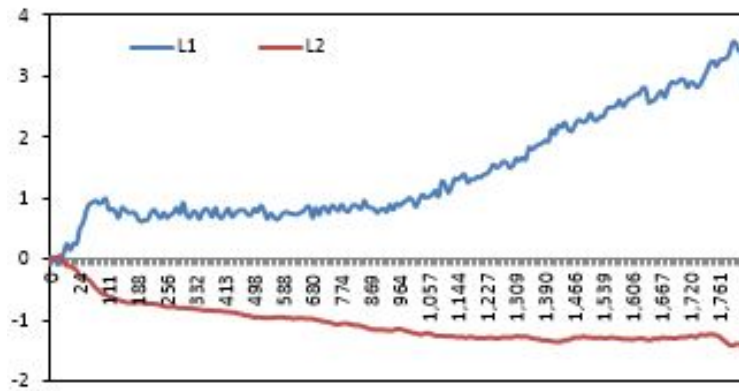


Figure 5.4: The mid-span expansion of the C1-0 specimen.

It can be seen from figure 5.4, above, that this specimen had a larger expansion in one direction compared to the other direction. This was not the case however, as the expansion of the specimens mid-span was uniform. This increase in the expansion indicates the presence of off-centre loading towards the new laser. The graph showing the mid-span expansion of the C1-50 specimen can be seen below.

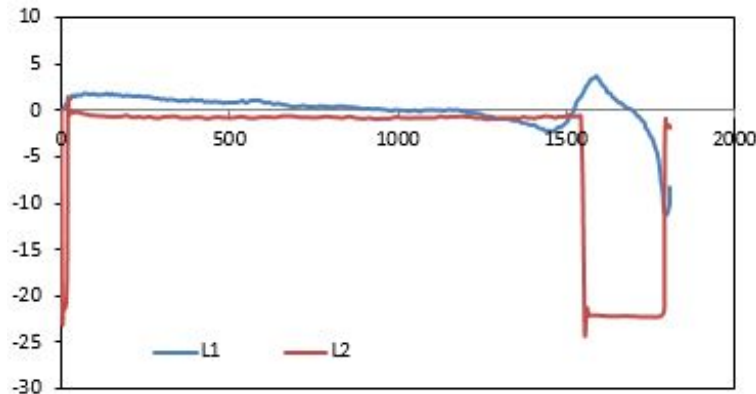


Figure 5.5: The mid-span expansion of the C1-50 specimen.

It can be seen from figure 5.5, above, that the mid-span expansion of this specimen was much more confined than the C1-0 specimen. It can be seen that there is no buckling evident with this specimen as both expansions are relatively constant. The sudden decrease in distance between the specimen and the two lasers can be explained by the laser being moved by debris that occurred after the cover concrete spalled, which resulted in some shattering. The graph showing the mid-span expansion of the C1-100 specimen can be seen below.

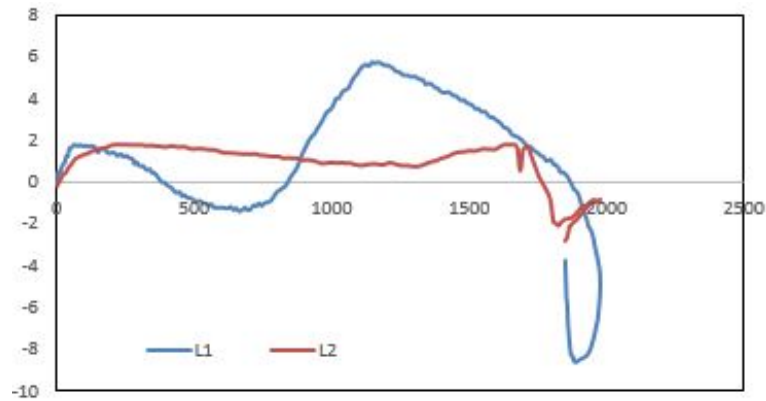


Figure 5.6: The mid-span expansion of the C1-100 specimen.

It can be seen that the C1-100 specimen, figure 5.6 above, had what appears to be a uniform expansion across the mid-section. It can be seen that one of the lasers, recorded as the new laser, expanded to 2mm, with the application of the load, however as the loading continued to be applied, the expansion of the centre of the column effectively ceased. When this is compared to the reading obtained from the other laser, a large variance can be seen. When this reading is combined with the strain graphs reported in chapter 4, it can be seen that there may have been some buckling occurring within this specimen. Another reason for this variance is that the compressive loading may have been applied slightly off centre, which results in more strain within one bar. The graph showing the mid-span expansion of the C1-200 specimen can be seen below.

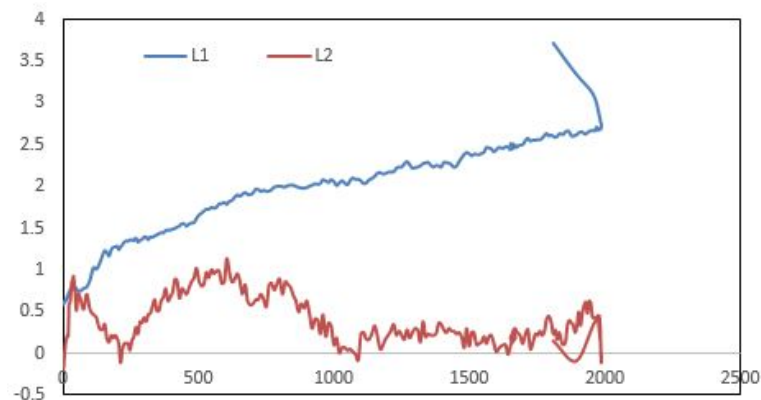


Figure 5.7: The mid-span expansion of the C1-200 specimen.

In figure 5.7, above, it can be seen that the laser, marked as the new laser, had some initial expansion when the load is applied before returning to zero. This can be put down to the specimen rocking when the loading was initially applied. After this, it can be seen that the mid-section of the specimen again increased, before gradually decreasing and remaining around 0.5mm. The graph labelled as the old laser however consistently

increased until the failure of the specimen. This behaviour can be explained when the graph of the strain in the longitudinal bars and external concrete strain is included. It can be seen that this increase of distance can be credited to a combination of buckling as well as the loading being applied slightly off centre.

The mid span expansions of each specimen cannot be compared together due a variety of factors. These factors include: the non-homogenous behaviour of the geopolymer concrete, along with the failure not being always being at the location that the lasers were recording from.

This study is unique as it also takes into account the effect of the longitudinal bars on the strength of the specimen. The percentage increase in strength can be calculated through the use of equation 5.1, below.

$$Contribution(\%) = \varepsilon_{peak} * E * A_b / P_{max} * 100 \quad (5.1)$$

The contribution of the longitudinal bars for the specimens transversely reinforced by hoop ties can be seen below in table 5.1.

Table 5.1: The percentage increase in strength contributed by the longitudinal bars for specimens with hoop ties.

Specimen	% contribution of bars (initial peak)	% contribution of bars (second peak)
C1-0	6.95	-
C1-50	8.52	24.14
C1-100	6.71	-
C1-200	6.78	-

It can be seen from the above table that the longitudinal bars contributed between 6.7-8.5% of the total compressive strength of the specimens reinforced with hoop ties. It should be noted that as the spacing of the transverse reinforcement was decreased the contribution of the longitudinal bars was increased, with the exception of the C1-50 specimen. This was because of the specimen having the core effectively confined so that the entire specimen was able to take an increase in loading. It was found that the use of GFRP bars as longitudinal reinforcement is acceptable. This is due to GFRP bars nearing the contribution of steel bars which contribute approximately 12% of the compressive

strength of the specimen.

5.2.2 Spacing of Spiral Ties

Similarly, the graphs of the strain recorded in the longitudinal bars and transverse ties for the specimens C1-0, S1-50 and S1-100 ties are shown below in figures 5.8 and 5.9 respectively.

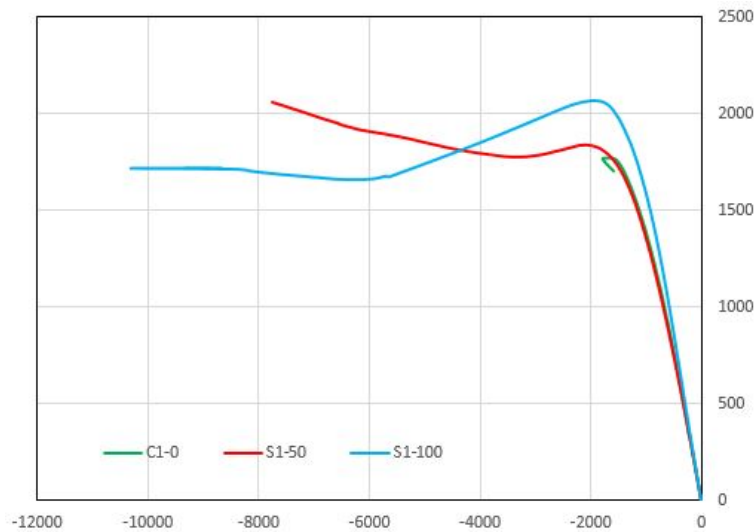


Figure 5.8: The average strain carried by the longitudinal bars transversely reinforced by spiral ties.

As previously stated, the C1-0 specimen, behaved as expected, having the lowest resistance to the loading, as well as carrying the smallest amount of strain within the longitudinal bars, seen above in figure 5.8. It can be seen that when spiral ties were introduced, the load capacity was enhanced, with the new ultimate load being approximately 2000kN. It was also observed that the S1-50 specimen had a peak loading that was less than the other specimens that were reinforced with spiral ties, which was not predicted. This was a result of the way this specimen was cast. As the spiral ties were close so closely spaced, the geopolymer concrete did not pass through the ties to create an effective cover despite meeting all vibratory requirements during casting. Another reason for the lower strain within the S1-50 specimen was the progressive failure of the S1-100 specimen due to this specimens weaker core.

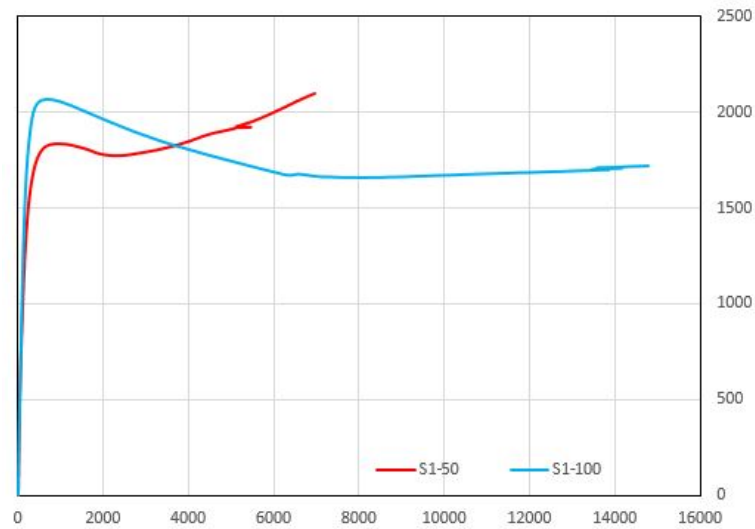


Figure 5.9: The average strain carried by spiral ties.

As observed with the transverse strain for the specimens reinforced by hoop ties, the S1-100 specimen had a higher strain than the S1-50 specimen, figure 5.9. It was observed that this specimen had an increase in the loading after the initial peak loading. This specimen had a peak loading of approximately 2200kN, which was a result of the spiral tie being a continuous piece of reinforcement, which allowed the strain to be transferred throughout the entire specimen instead of localising the strain in a particular area. This agrees with the findings of the Leung and Burgoyne study findings.

It can be seen from figures 5.8 and 5.9, both above, that there is a linear load-strain relationship until a loading of approximately 1800kN, which was when the spalling of the concrete cover occurred. After this, the loading slightly increases to approximately 2000kN before not changing while the strain is increased. This occurred due to the concrete core taking most of the loading.

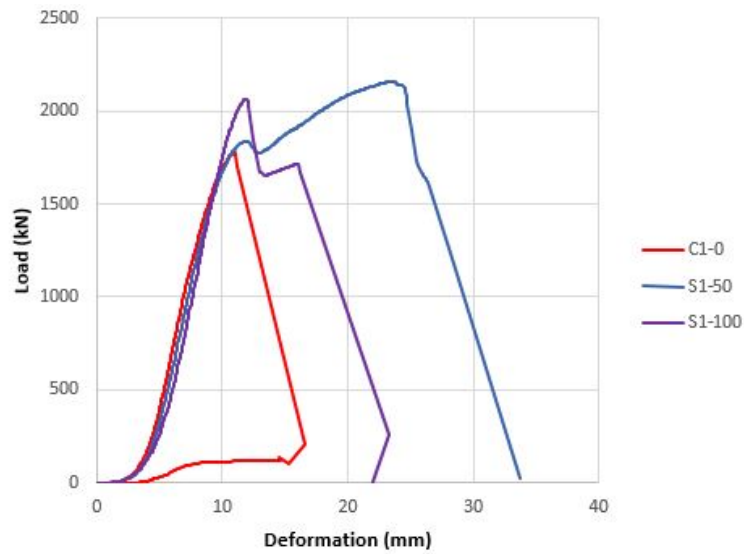


Figure 5.10: The compressive deflection of the specimens reinforced with a spiral tie.

It can be seen from figure 5.10 that the addition of a spiral transverse tie increased both the ductility and the ultimate loading capacity of the specimen. Once again the specimen that had a spacing of 50mm had a lower initial peak load compared to the specimen with a 100mm spacing. Once again, this was because of the concrete not being able to pass between the small spacing between the ties, which prevented continuity of the concrete within the specimen. The S1-50 spacing however resulted in a larger peak loading in the end due to the effect of the confinement of the core of the specimen. . In the S1-50 and S1-100 specimens a second peak is evident. This second peak can be calculated using the loading at the peak, along with the cross sectional area of the core, due to the cover concrete having spalled. The loading that this peak occurs at is dependent on how effectively the core of the specimen is confined. The mid-span expansion was also recorded, through the use of two lasers, placed at right angles to each other. The graph showing the mid-span expansion of the C1-0 specimen can be seen below.

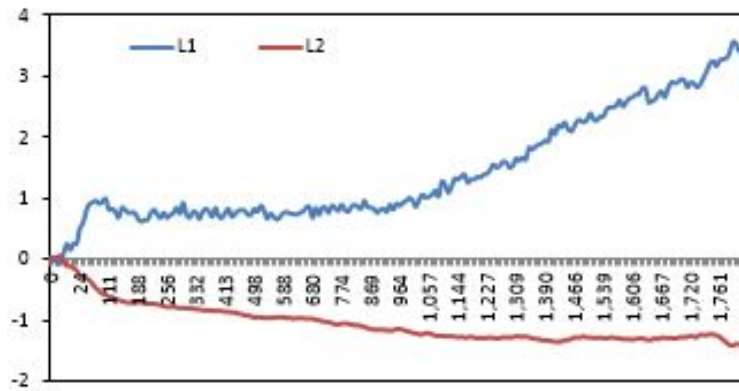


Figure 5.11: The mid-span expansion of the C1-0 specimen.

It can be seen from figure 5.11, above, that this specimen had a larger expansion in one direction compared to the other direction. This was not the case however, as the expansion of the specimens mid-span was uniform. This increase in the expansion indicates the presence of off-centre loading towards the new laser. The graph showing the mid-span expansion of the S1-50 specimen can be seen below.

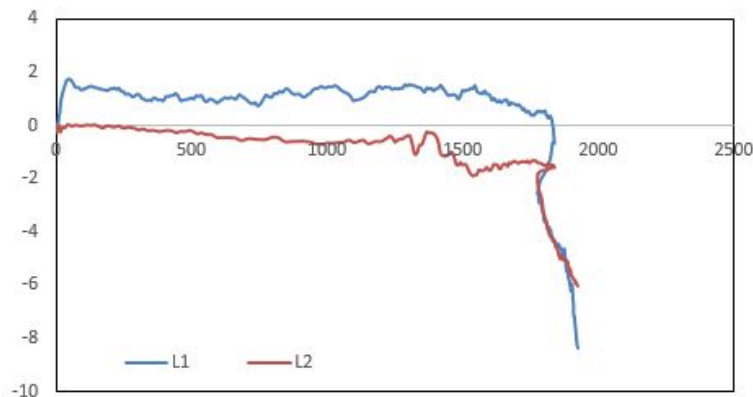


Figure 5.12: The mid-span expansion of the S1-50 specimen.

It can be seen in figure 5.12, above, that both lasers recorded an expansion of the mid-section. This was until a loading of approximately 1800kN. This was the loading that spalling of the cover occurred, which when cracking could have resulted in the laser being hit by shattered debris, changing the point the laser was aimed at causing this drop in distance at the end of the graph. The graph showing the mid-span expansion of the S1-100 specimen can be seen below.

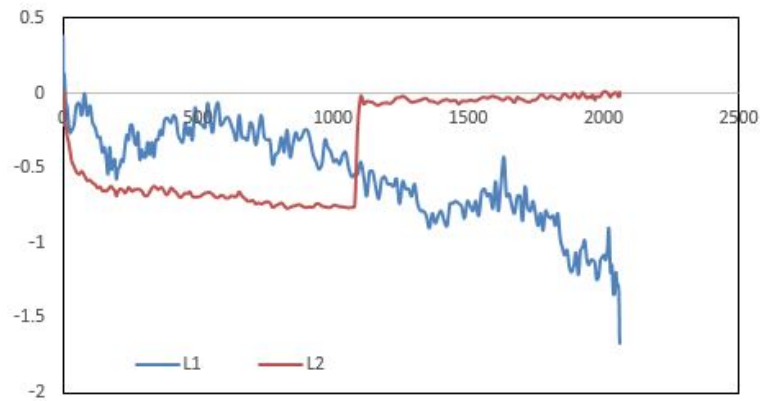


Figure 5.13: The mid-span expansion of the S1-100 specimen.

It can be seen from the above figure, figure 5.13, that the laser labelled the old laser recorded a steady increase in the diameter of the sections mid-span, after an initial movement from the load initially being applied. The other laser, labelled the new laser, recorded an abnormal movement. It can be seen that the mid-span increases as the load is increased, however at approximately 1000kN the mid-span returns to the initial position. This could be because of numerous reasons. A void in the surface of the specimen could have cause the laser to return to the initial reading if the expansion caused the void to cross the lasers path. Another explanation for this anomaly is that the mid-span expansion moved outside the lasers range, giving a zero reading for the remained of the testing of this specimen.

Once again, the mid span expansions of each specimen cannot be compared together due a variety of factors. These factors include: the non-homogenous behaviour of the geopolymer concrete, along with the failure not being always being at the location that the lasers were recording from.

Similarly, the contribution of the longitudinal bars for the specimens transversely reinforced by spiral ties can be seen below in table 5.2.

Table 5.2: The percentage increase in strength contributed by the longitudinal bars for specimens with spiral ties.

Specimen	% contribution of bars (initial peak)	% contribution of bars (second peak)
C1-0	6.95	-
S1-50	8.13	28.13
S1-100	7.13	-

It can be seen from the above table that the longitudinal bars contributed between 6.95-8.13% of the total compressive strength of the specimens reinforced with spiral ties. Unlike the specimens reinforced with hoop ties, the contribution of the longitudinal bars was increased as the spacing of the transverse ties was decreased. Once again, it was found that the use of GFRP bars as longitudinal reinforcement is acceptable. This is due to GFRP bars nearing the contribution of steel bars which contribute approximately 12% of the compressive strength of the specimen.

5.2.3 Summary of the Effect of Spacing

It was also observed that the spacing did have an effect on the overall behaviour of the specimen. This was because of the rate of failure of the specimens. It was observed that as the spacing between the transverse ties was reduced, the amount of strain present in the specimen increase, along with decreasing the specimens ability to resist loading. It can be seen that the inclusion of transverse reinforcement results in an increase in the load capacity and the amount of strain carried by the specimen. It could be seen that for both types of transverse reinforcement that the specimens that had a spacing of 50mm had a lower peak load compared to the other specimens that were transversely reinforced. This was because of the higher amount of reinforcement stopping the continuity of the concrete. The effect of spacing also had an effect of the amount of strain present within the longitudinal bars and transverse ties. It was observed that the specimens with a spacing of 100mm resulted in a higher strain within the transverse ties. This was because of the larger spacing between the transverse ties, resulting in a larger strain present in the ties. It can also be seen that the C1-50 specimen recorded a larger strain within the longitudinal bars that all other specimens reinforced with hoop ties. This pattern however was not observed within the specimens that had a spiral tie as the type of transverse reinforcement. This was because of the spiral ties distributing the strain evenly throughout the specimen

instead of localising the strain in an area.

5.3 Effect of Type of Transverse Reinforcement

The type of transverse reinforcement used can also effect the behaviour of the specimen. Due to the design of the spiral specimen, any strain carried will be transferred throughout the entire specimen, instead of being localised, which is the case for the hoop ties. To properly analyse the effect of the type of transverse reinforcement, specimens will be separated into groups with the same spacing, regardless of the transverse reinforcement type. Within these two groups, the strain that was carried by the longitudinal bars as well as the transverse bars will be analysed.

5.3.1 Spacing of 50mm

Figures 5.14 and 5.15, below, show the average strain carried by the longitudinal and transverse bars, for specimens: C1-0, C1-50 and S1-50, respectively.

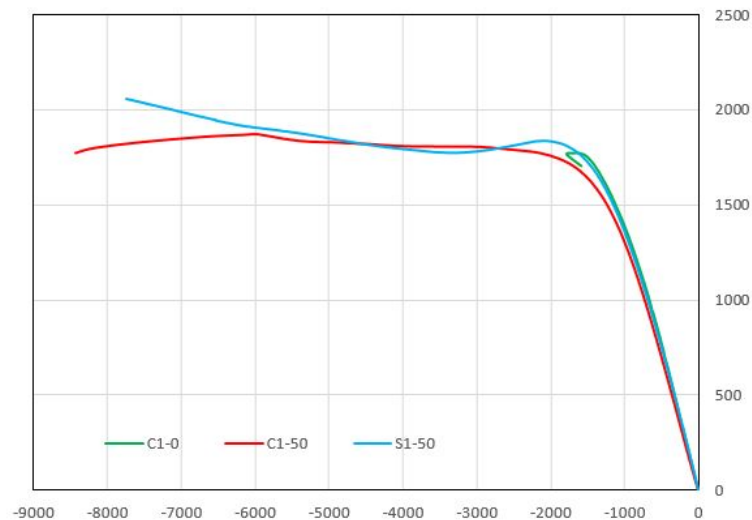


Figure 5.14: The strain carried in the longitudinal bars of specimens that had a spacing of 50mm.

It can be seen in figure 5.14 that all specimens began spalling at a load of approximately 1800kN. As predicted, both the specimens that had a spacing of 50mm carried significantly larger amount of strain compared to the control specimen. It can be seen that both types of reinforcement carried a strain of approximately 8000, however the specimen reinforced

with hoop ties were able to carry a larger strain. This is because the hoop ties localised the strain onto the longitudinal bars, while the spiral tie retained most of the strain within the transverse reinforcement. It can also be seen that the specimen reinforced with the spiral tie was able to withstand a higher loading.

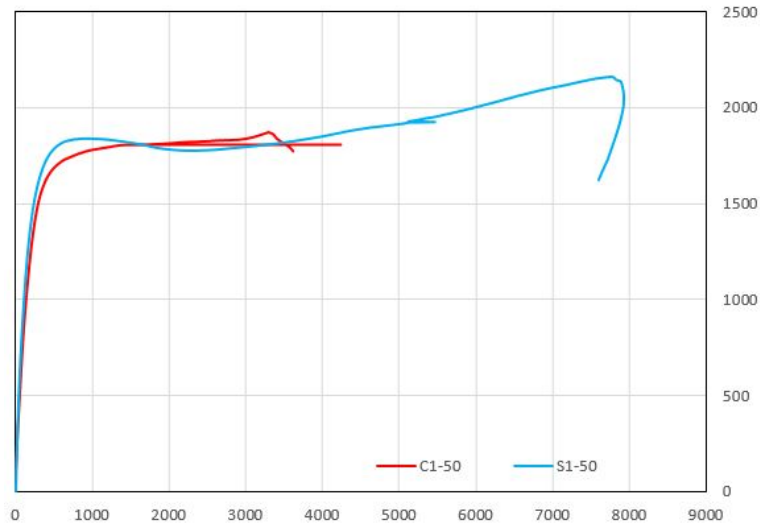


Figure 5.15: The strain carried in the transverse reinforcement of specimens that had a spacing of 50mm.

The control specimen was again left out of the transverse reinforcement analysis, due to not having any transverse reinforcement. It can be seen from figure 5.15, above, that both specimens had the cover spall at approximately the same loading, however the spiral specimen carried almost twice as much strain as the hoop ties. This was because to the transverse reinforcement expanded as the column was compressed, which caused the hoop ties to expand past the overlapped length, and after this point, became ineffective in confining the specimen, while the spiral tie spread the strain throughout the entire specimen.

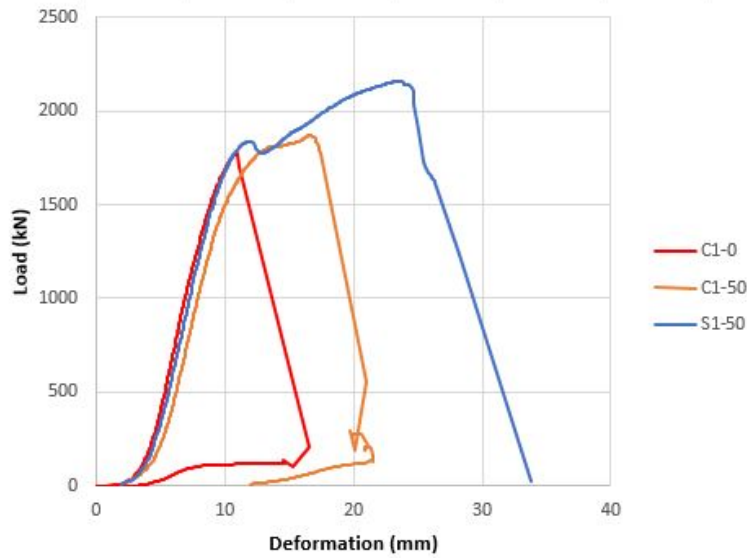


Figure 5.16: The compressive deflection of the specimens reinforced with a spacing of 50mm.

It can be seen from figure 5.16, above, that both types of transverse reinforcement resulted in an increase in both the ultimate load carrying capacity and ductility of the specimens. It can be seen that the specimen that was reinforced by the spiral tie was able to carry by the largest ultimate load, along with having the largest deformation of the specimens. The mid-span expansion has also been recorded for comparison. The graph showing the mid-span expansion of the C1-0 specimen can be seen below.

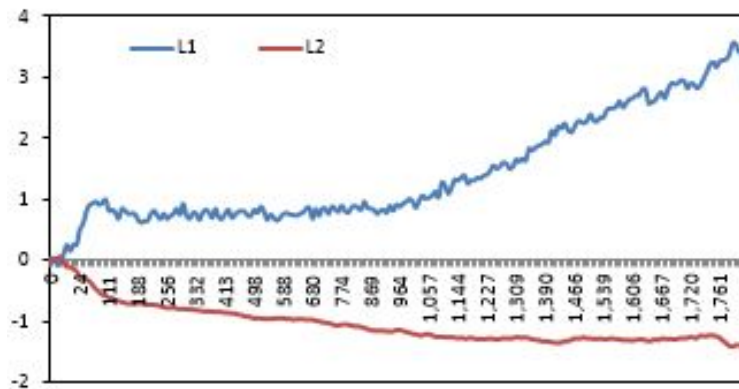


Figure 5.17: The mid-span expansion of the C1-0 specimen.

It can be seen from figure 5.17, above, that this specimen had a larger expansion in one direction compared to the other direction. This was not the case however, as the expansion of the specimens mid-span was uniform. This increase in the expansion indicates the presence off centre loading towards the new laser. The graph showing the mid-span expansion of the C1-50 specimen can be seen below.

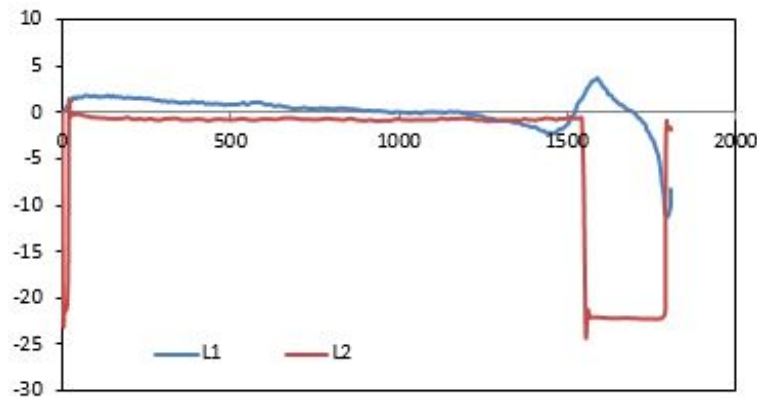


Figure 5.18: The mid-span expansion of the C1-50 specimen.

It can be seen from figure 5.18, above, that the mid-span expansion of this specimen was much more confined than the C1-0 specimen. It can be seen that there is no buckling evident with this specimen as both expansions are relatively constant. The sudden decrease in distance between the specimen and the two lasers can be explained by the laser being moved by debris that occurred after the cover concrete spalled, which resulted in some shattering. The graph showing the mid-span expansion of the S1-50 specimen can be seen below.

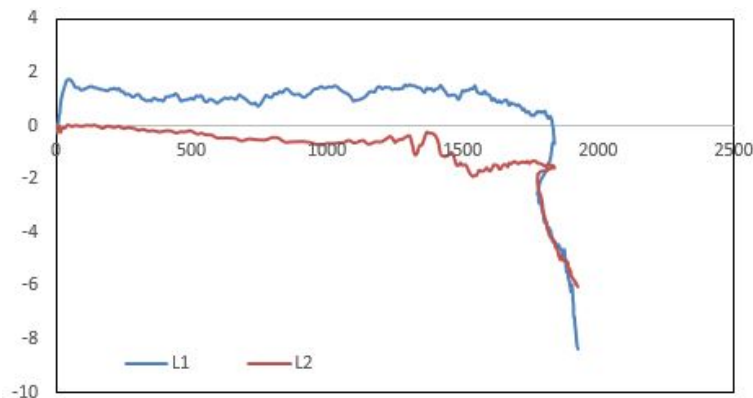


Figure 5.19: The mid-span expansion of the S1-50 specimen.

It can be seen in figure 5.19, above, that both lasers recorded an expansion of the mid-section. This was until a loading of approximately 1800kN. This was the loading that spalling of the cover occurred, which when cracking could have resulted in the laser being hit by shattered debris, changing the point the laser was aimed at causing this drop in distance at the end of the graph. The graph showing the mid-span expansion of the S1-100 specimen can be seen below.

Once again, the mid span expansions of each specimen cannot be compared together

due a variety of factors. These factors include: the non-homogenous behaviour of the geopolymer concrete, along with the failure not being always being at the location that the lasers were recording from.

To properly compare the difference between the hoop and spiral ties, the contribution of the longitudinal bars for the specimens that had a spacing of 50mm for the transverse reinforcement can be seen below in table 5.3.

Table 5.3: The percentage increase in strength contributed by the longitudinal bars for specimens with a spacing of 50mm.

Specimen	% contribution of bars (initial peak)	% contribution of bars (second peak)
C1-0	6.95	-
C1-50	8.52	24.14
S1-50	8.13	28.13

It can be seen from table 5.3, above, that for the specimens with a transverse spacing of 50mm each had a contribution to the total strength that was in excess of 8%. The C1-50 specimen had a larger contribution due to the hoop ties placing a large amount of the strain back on the longitudinal bars, while the spiral tie transferred most of the strain in the transverse direction, as seen previously in figure 5.15. Once again it can be seen that both specimens had a contribution from the longitudinal bars that were neat the contribution of steel longitudinal bars. It can also be seen that the specimen that was reinforced with a spiral tie had a larger contribution in regards to the second peak loading of the specimen. This was because the spiral tie allowed the strain to be transferred over the entire specimen, which in turn allowed for a higher loading and observed strain.

5.3.2 Spacing of 100mm

Similarly, the specimens C1-0, C1-100 and S1-100 can be analysed in the same way. The graphs of the strain carried within the longitudinal bars and transverse reinforcement are shown below in figures 5.20 and 5.21 respectively.

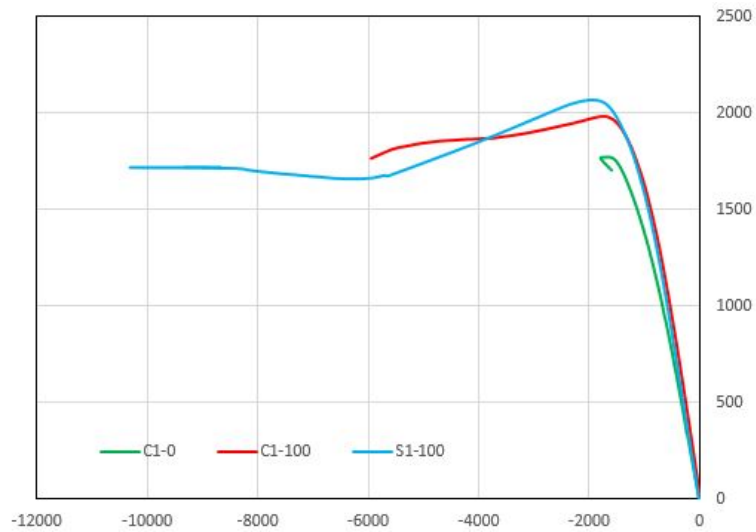


Figure 5.20: The strain carried in the longitudinal bars of specimens that had a spacing of 100mm.

It can be seen in figure 5.20, above, that the C1-0 specimen once again withstood the lowest loading as well as carrying the smallest amount of strain. It can be seen that both the C1-100 and S1-100 specimens had a peak loading of approximately 2000kN, however the S1-100 specimen carried a significantly higher strain than the C1-100 specimen. This is because of the previously mentioned reason that the failure of the S1-100 specimen was more progressive than the other specimens due to a weaker core.

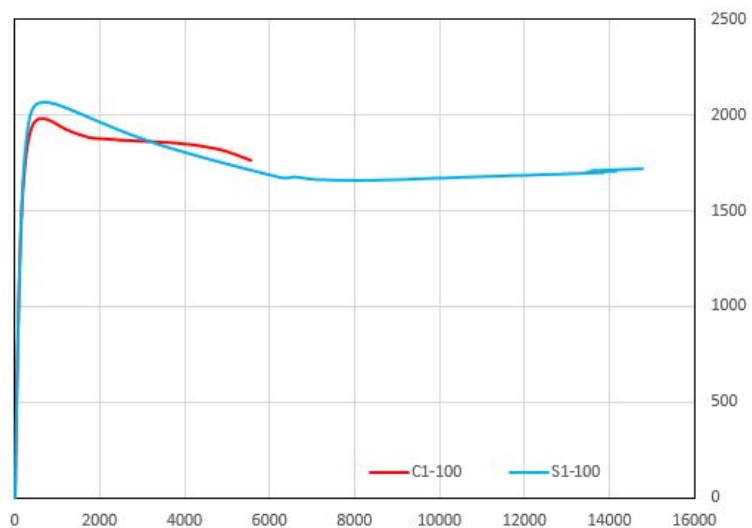


Figure 5.21: The strain carried in the transverse reinforcement of specimens that had a spacing of 100mm.

Once again, the control specimen was left out of the transverse reinforcement analysis, due to not having any transverse reinforcement. It can be seen from figure 5.21, above, that both specimens had the cover spall at approximately the same loading, however the

spiral specimen carried more than double the amount of strain present in the hoop ties. Once again, this was because to the transverse reinforcement expanded as the column was compressed, which caused the hoop ties to expand past the overlapped length, and after this point, became ineffective in confining the specimen, while the spiral tie spread the strain throughout the entire specimen.

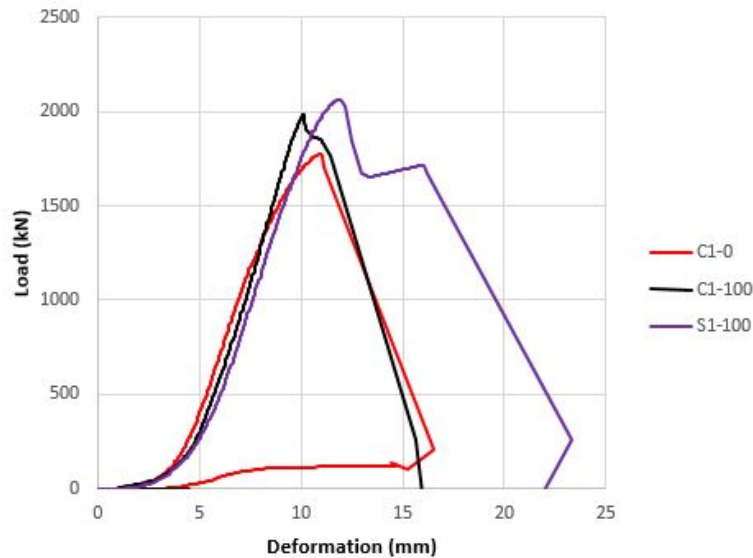


Figure 5.22: The compressive deflection of the specimens reinforced with a spacing of 100mm.

It can be seen from figure 5.22, above, that both types of transverse reinforcement resulted in an increase in both the ultimate load carrying capacity and ductility of the specimens. Once again, it can be seen that the specimen that was reinforced by the spiral tie was able to carry the largest ultimate load, along with having the largest deformation of the specimens, however, unlike the specimens that have a spacing of 50mm, the difference between the ultimate loads of the two types of transverse reinforcement is minimal. The mid-span expansion has also been recorded for comparison. The graph showing the mid-span expansion of the C1-0 specimen can be seen below.

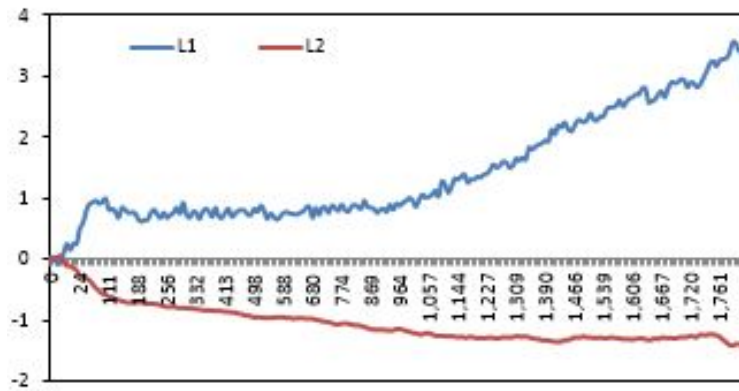


Figure 5.23: The mid-span expansion of the C1-0 specimen.

It can be seen from figure 5.23, above, that this specimen had a larger expansion in one direction compared to the other direction. This was not the case however, as the expansion of the specimens mid-span was uniform. This increase in the expansion indicates the presence off centre loading towards the new laser. The graph showing the mid-span expansion of the C1-100 specimen can be seen below.

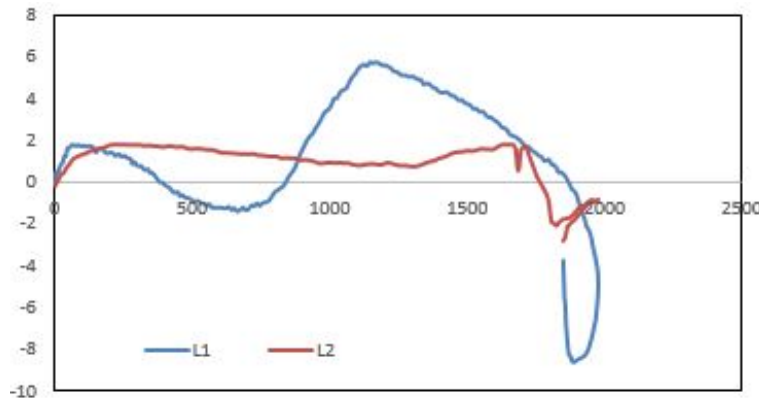


Figure 5.24: The mid-span expansion of the C1-100 specimen.

It can be seen that the C1-100 specimen, figure 5.24 above, had what appears to be a uniform expansion across the mid-section. It can be seen that one of the lasers, recorded as the new laser, expanded to 2mm, with the application of the load, however as the loading continued to be applied, the expansion of the centre of the column effectively ceased. When this is compared to the reading obtained from the other laser, a large variance can be seen. When this reading is combined with the strain graphs reported in chapter 4, it can be seen that there may have been some buckling occurring within this specimen. Another reason for this variance is that the compressive loading may have been applied slightly off centre, which results in more strain within one bar. The graph showing the mid-span expansion of the S1-100 specimen can be seen below.

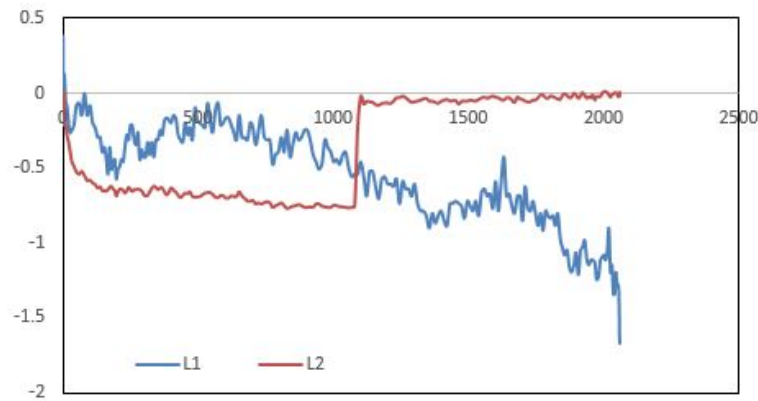


Figure 5.25: The mid-span expansion of the S1-100 specimen.

It can be seen from the above figure, figure 5.25, that the laser labelled the old laser recorded a steady increase in the diameter of the sections mid-span, after an initial movement from the load initially being applied. The other laser, labelled the new laser, recorded an abnormal movement. It can be seen that the mid-span increases as the load is increased, however at approximately 1000kN the mid-span returns to the initial position. This could be because of numerous reasons. A void in the surface of the specimen could have cause the laser to return to the initial reading if the expansion caused the void to cross the lasers path. Another explanation for this anomaly is that the mid-span expansion moved outside the lasers range, giving a zero reading for the remained of the testing of this specimen.

As per the specimens with a spacing of 50mm, the mid span expansions of each specimen cannot be compared together due a variety of factors. These factors include: the non-homogenous behaviour of the geopolymer concrete, along with the failure not being always being at the location that the lasers were recording from.

To properly compare the difference between the hoop and spiral ties, the contribution of the longitudinal bars for the specimens that had a spacing of 100mm for transverse reinforcement can be seen below in table 5.4.

Table 5.4: The percentage increase in strength contributed by the longitudinal bars for specimens with a spacing of 100mm.

Specimen	% contribution of bars (initial peak)	% contribution of bars (second peak)
C1-0	6.95	-
C1-100	6.71	-
S1-100	7.12	-

It can be seen from table 5.4, above, that for the specimens with a transverse spacing of 100mm each had a contribution to the total strength that between 6.7 and 7.15%. Unlike the specimens with a spacing of 50mm, the S1-100 specimen had the largest contribution from the longitudinal bars at 7.12%. This was despite the strain being transferred into the transverse direction as the observed failure of this specimen was much more gradual than all other specimens. Once again it can be seen that both specimens had a contribution from the longitudinal bars that was close to the contribution of steel longitudinal bars.

5.3.3 Summary of the Effect of the Type of Transverse Reinforcement

It was also observed that the type of transverse reinforcement did have an effect on the overall behaviour of the specimen. This was because of the rate of failure of the specimens. It was observed that as the specimens reinforced with a spiral allowed for a larger amount of strain to be carried by the specimen, a higher load carrying capacity, as well as a larger compressive deflection. It can be seen that the inclusion of transverse reinforcement results in an increase in the load capacity and the amount of strain carried by the specimen. It could be seen that for both types of transverse reinforcement that the specimens that had a spacing of 50mm had a lower peak load compared to the other specimens that were transversely reinforced. This was because of the higher amount of reinforcement stopping the continuity of the concrete. The effect of transverse ties also had an effect of the amount of strain present within the longitudinal bars and transverse ties. It was observed that the specimens with a spacing of 50mm recorded similar strain within the longitudinal bars, however the S1-50 specimen resulted in a much larger strain in the transverse direction. It can also be seen that the S1-100 specimen also recorded a larger strain within both the longitudinal bars and transverse ties when compared to the C1-100 specimen.

5.4 Theoretical Analysis

This section uses equations found from literature and existing standards to theoretically predict the specimens behaviour. To accurately do this, 4 equations have been found to use from the works of: Afifi (Afifi et al. 2014) and Mohamed (Mohamed et al. 2014). The four equations that were used can be seen below:

$$P_o = \alpha_1 * f_c * (A_g - A_f) \quad (5.2)$$

$$P_o = 0.85 * f_c * (A_g - A_f) \quad (5.3)$$

$$P_o = 0.85 * f_c * (A_g - A_f) + \alpha_g * f_{fu} * A_f \quad (5.4)$$

$$P_o = 0.85 * f_c * (A_g - A_f) + \epsilon_{f-peak1-ave} * E_f * A_f \quad (5.5)$$

Where:

- $\alpha_1 = 0.85 - 0.0015 * f_c > 0.67 = 0.79342$
- f_c =specified compressive strength of concrete=37.72 MPa
- A_g =gross section of concrete=49087.39 mm^2
- A_f =area of FRP tension reinforcement=1191.339 mm^2
- α_1 =reduction factor of GFRP bars compressive strength=0.35
- f_{fu} =ultimate tensile strength of FRP reinforcement=1184 MPa
- $\epsilon_{f-peak1-ave}$ =strain at initial peak loading=0.002
- E_f =modulus of elasticity of FRP reinforcement=62.9 GPa

The results from these two equations can be seen below in table 5.5.

Table 5.5: The results that were obtained through the use of equations 5.2-5.5.

Equation	P_o (kN)
5.2	1433.423
5.3	1535.643
5.4	2029.334
5.5	1685.513

These values were then compared to the results obtained at the initial peak of by each of the specimens. These predictions are however still an inaccurate prediction. This is due to the strength reduction (α_1) value. This is because this relationship is calculated using relationships for Ordinary Portland Cement concrete rather than geopolymer concrete. To counteract this, different values of the α_1 were tried, with the results shown in table 5.6.

Table 5.6: The results yielded through different α_1 values.

α_1	equation 5.2 (kN)	equation 5.3 (kN)	equation 5.4 (kN)	equation 5.5 (kN)
0.85	1535.643	1535.643	2029.334	1685.513
0.86	1553.709	1553.709	2047.4	1703.58
0.87	1571.776	1571.776	2065.467	1721.646
0.88	1589.842	1589.842	2083.533	1739.713
0.89	1607.909	1607.909	2101.599	1757.779
0.90	1625.975	1625.975	2119.666	1775.845
0.91	1644.041	1644.041	2137.732	793.912
0.92	1662.108	1662.108	2155.799	1811.978
0.93	1680.174	1680.174	2173.865	1830.045
0.94	1698.241	1698.241	2191.931	1848.111
0.95	1716.307	1716.307	2209.998	1866.177

It can be seen that the equation that most accurately predicts the behaviour of all of the specimens is equation 5.5. This was due to the large variance in the initial peak loads, ranging from 1759.6 kN to 2062.8 kN. It was found that the strength reduction factor (α_1) value that best suits the initial peaks of all specimens was a value of 0.91. Therefore it is recommended that equation 5.5 is used to calculate the loading capacity of GFRP reinforced geopolymer concrete columns, while a strength reduction factor (α_1) of 0.91

should be used.

5.5 Conclusion

These results show that both GFRP hoop and spiral ties are effective in providing confinement to a GFRP reinforced geopolymer column. It can be seen that the S1-50 specimen was able to increase the peak load after the spalling of the concrete cover. This was due to the spiral tie being one continuous piece of reinforcement, and therefore distributing the strain throughout the entire specimen, which concurs with the findings of Leung and Burgoyne's findings. The results also show that the spiral ties are slightly more effective, due to having a higher ultimate load, ductility as well as confinement efficiency. These findings are why it is recommended that the spiral ties be used if GFRP reinforced geopolymer concrete is to be used within the construction industry. These results are in agreeance to the results obtained by the Mohamed, Afifi and Benmokrane study from 2014. As previously mentioned, this study differs from the previously mentioned studies as the effect of the longitudinal GFRP bars on the behaviour of the specimen has been included. It was calculated that the longitudinal bars resulted in an increase in strength between 6-9% of the entire specimen. This contribution from the longitudinal bars is not quite as much as the contribution of steel reinforcement (12%) but should not be neglected. It can also be seen that that equation 5.5 provides the most accurate prediction of the behaviour of GFRP reinforced geopolymer concrete. This accurate prediction can be obtained if a strength reduction factor (α_1) of 0.91 is used.

Chapter 6

Summary, Conclusions and Recommendation for Future Work

6.1 Summary

Reinforced concrete (RC) is one of the most popular construction materials. Columns are critical to the safety as well as the performance of the structure. RC columns traditionally use Portland cement as a main ingredient for the cement as well as using steel bars and stirrups for reinforcement. One major problem encountered by RC columns is the corrosion of the reinforcement cages. The corrosion of the steel cages can result in deterioration of the concrete, loss of serviceability as well as, in extreme cases, brittle failure of not only the column but the entire structure. This has resulted in the search for a product that will not corrode but still has the same effect on the strength and behaviour of the RC column. This search led to the trial of fibre reinforced polymer (FRP) material. The most common type of FRP used is glass fibre reinforced material (GFRP). GFRP is made from high strength glass fibres surrounded by polymer matrices and shaped in the form of bars, tubes and grids in a large variety of shapes and characteristics.

Another major problem is the issue of global warming. There is major concern over the amount of CO_2 released by Portland cement during the curing process. Due to modern day societies being extremely environmentally conscientious, an alternative product is needed to reduce this amount. Until a suitable replacement is found, multiple materials are being used in an effort to decrease the amount of Portland cement. This has resulted

in the product which is known as geopolymer cement. Geopolymer concrete has been used in many projects around the world, and has been found to have the same strength as concrete.

To test these two promising construction materials in combination, six specimens were created, with the parameters of spacing between transverse reinforcement and type of transverse reinforcement varied. Each specimen was then tested through the application of axial loading with the internal longitudinal strain, internal transverse strain, external concrete strain and deformation observed in each specimen recorded.

The obtained results stated that both GFRP hoop and spiral ties are effective in providing confinement to a GFRP reinforced geopolymer column. It could be seen that the S1-50 specimen was able to increase the peak load after the spalling of the concrete cover. This was due to the spiral tie being one continuous piece of reinforcement, and therefore distributing the strain throughout the entire specimen, which concurs with the findings of Leung and Burgoyne's findings. The results also show that the spiral ties are slightly more effective, due to having a higher ultimate load, ductility as well as confinement efficiency. These findings are why it is recommended that the spiral ties be used if GFRP reinforced geopolymer concrete is to be used within the construction industry. These results are in agreement to the results obtained by the Mohamed, Afifi and Benmokrane study from 2014. This study differs from the previously mentioned studies as the effect of the longitudinal GFRP bars on the behaviour of the specimen has been included. It was calculated that the longitudinal bars resulted in an increase in strength between 6-9% of the entire specimen. This contribution from the longitudinal bars is not quite as much as the contribution of steel reinforcement (12%) however, are still significant enough to avoid being neglected. It was also found that that equation 5.5 provides the most accurate prediction of the behaviour of GFRP reinforced geopolymer concrete. This equation does not result in an accurate prediction of the capacity of the specimens. This was due to the strength reduction factor (α_1) used being calculated for ordinary Portland cement concrete. An accurate prediction can be obtained if a strength reduction factor of 0.91 is used.

6.2 Conclusions

Based on the experimental and theoretical data that was obtained throughout the research, the following conclusions can be drawn from the research program:

6.2.1 Spacing of Transverse Reinforcement

1. The spacing of the transverse ties did have an effect on the overall behaviour of the specimens, by allowing for a higher loading (increase of approximately 15kN on average) and greater strain carrying capacity (increased by approximately 275 microstrain).
2. Despite the C1-100 and C1-200 having the same peak load, spacing did effect the rate of failure as the C1-100 specimen was capable of resisting the loading for a larger period of time compared to the C1-200 specimen.
3. It could be seen that for both types of transverse reinforcement that the specimens that had a spacing of 50mm had a lower peak load, a drop approximately 110kN less, when compared to the control specimen C1-0.

6.2.2 Type of Transverse Reinforcement

1. It was observed that the type of transverse reinforcement did have an effect on the overall behaviour of the specimen. It was observed that as the specimens reinforced with a spiral allowed for a larger amount of strain (6000 microstrain) to be carried by the specimen, a higher load carrying capacity (increase of approximately 175kN), as well as a larger compressive deflection (11mm on average) when compared to C1-0.

6.2.3 General Conclusions Reached From Experimental Results

1. It was found that the contribution of the longitudinal bars ranged between 6.71% and 8.52% for hoop ties and 6.95% and 8.13% for specimens reinforced with a spiral tie.

6.2.4 Theoretical Analysis

1. It can be seen that the equation that most accurately predicts the behaviour of all of the specimens is as follows: $P_o = 0.85 * f_c * (A_g - A_f) + \epsilon_{f-peak1-ave} * E_f * A_f$. This equation considers the concrete compressive strength, area of concrete in compression, longitudinal strain recorded at the peak loading, the Modulus of Elasticity of the GFRP bars, as well as the area of the GFRP bars used.
2. It was found that the strength reduction factor (α_1) value that best suits the initial peaks of all specimens was a value of 0.91. This value was determined as it provided the most accurate prediction of the peak loading of all six specimens.

6.3 Recommendations for Future Work

Based on the findings of this study, it can be seen that GFRP reinforced geopolymer concrete is suitable for use within the construction industry within Australia and therefore it is important to continue research studies in this promising field. Some of the recommendations for future areas of research are:

1. Investigation into the effect on slender columns.
2. Performing tests on specimens with rectangular cross sections.
3. Performing tests under different loading situations, such as seismic loading.
4. Testing the effect of the strength of the geopolymer concrete

References

- ACI (2006), Guide for the Design and Construction of Structural Concrete Reinforced with FRP Bars, Standard ACI 440.1R-06, American Concrete Institute.
- Afifi, M. (2013), 'Behaviour of Circular Concrete Columns Reinforced with FRP Bars and Stirrups', http://www.usherbrooke.ca/genie/fileadmin/sites/genie/documents/Intranet/theses_memoires/Afifi_M_20140121.pdf. [Online; accessed January-2015].
- Afifi, M. Z., Mohamed, H. M. & Benmokrane, B. (2014), 'Axial Capacity of Circular Concrete Columns Reinforced with GFRP Bars and Spirals', *ASCE Journal of Composites for Construction* **18**(1), 04013017–1–04013017–11.
- Akhilesh, P., Marepally, V. R. & Padmakanth, P. (2015), 'Geopolymer Concrete', <http://www.slideshare.net/akhileshpadiga/geo-polymer-concrete>. [Online; accessed May-2015].
- AS (2009), Concrete Structures, Standard AS 3600-2009, Sandards Australia.
- Bing, L., Park, R. & Tanaka, H. (2001), 'Stress-Strain Behaviour of High-Strength Concrete Confined by Ultra-High- and Normal-Strength Transverse Reinforcements', *ACI Structural Journal* **98**(3), 395–406.
- Bjerkeli, L., Romaszewicz, A. & Jensen, J. J. (1990), 'Deformation Properties and Ductility of High-Strength Concrete', *ACI Structural Journal* **121**(1), 215–238.
- CSA (2006), Canadian Highway Bridge Design Code, Standard CSA S806-12, Canadian Sandards Association.
- CSA (2012), Design and construction of building structures with fibre-reinforced polymers, Standard CSA S806-12, Canadian Sandards Association.

- Davidovits, J. (1994), 'Properties of Geopolymer Cements', http://www.geopolymer.org/fichiers_pdf/KIEV.pdf. [Online; accessed April-2015].
- Deb, A. (2015), 'Size effect in concrete under compression', <http://www.iitk.ac.in/tkic/slides/pravartana13/solid%20mechanics/effect%20of%20specimen.pdf>. [Online; accessed April-2015].
- Deitz, D. H., Harik, I. E. & Gesund, H. (2013), 'Physical Properties of Glass Fiber Reinforced Polymer Rebars in Compression', *ASCE Journal of Composites for Construction* **7**(4), 363–366.
- Edge, E. (2015), 'Yield Strength-Strength (Mechanics) of Materials', http://www.engineersedge.com/material_science/yield_strength.htm. [Online; accessed June-2015].
- Fam, A. Z. & Rizkalla, S. H. (2015), 'Concrete-Filled FRP Tubes for Flexural and Axial Compression Members', http://www.ce.ncsu.edu/srizkal/linked_files/2.pdf. [Online; accessed April-2015].
- Farahmand, F. (1996), 'Shear Behaviour of Concrete Beams Reinforced with Glass Fiber Reinforced Plastic', http://www.ce.ncsu.edu/srizkal/linked_files/Shear_Behavior_of_Concrete_Beams_Reinforced.pdf. [Online; accessed April-2015].
- Foster, S. J., Kilpartick, A. E. & Warner, R. F. (2010), *Reinforced Concrete Basics Second Edition*, Pearson.
- Hossain, K. M. A., Ametrano, D. & Lachemi, M. (2014), 'Bond Strength of Standard and High-Modulus of GFRP Bars in High-Strength Concrete', *ASCE Journal of Materials in Civil Engineering* **26**(3), 449–456.
- Hughes Brothers, I. (2011), 'Reinforced Polymer (GFRP) Rebar - Aslan 100 series', <http://www.aslanfrp.com/Media/Aslan100.pdf>. [Online; accessed March-2015].
- Hughes Brothers, I. (2015), 'Glass Fiber Reinforced Polymer (GFRP) Rebar', <http://www.hughesbros.com/Aslan100%20GFRP.pdf>. [Online; accessed April-2015].
- Improvement, M. H. (2015), 'Hardaz Aviary Wire Mesh 25x25x1.24mm 90cmx30m', <https://www.masters.com.au/product/900033341/hardaz-aviary-wire-mesh-25x25x1-24mm-90cm-x-30m>. [Online; accessed August-2015].

- Iran, A. (2015), 'GFRP (Glass Fiber Reinforced Polymer) Rebar', http://rustrade.org.uk/eng/wp-content/uploads/ARMASTEK_GFRP_Presentation.pdf. [Online; accessed April-2015].
- Leung, H. Y. & Burgoyne, C. J. (2001), 'Compressive Behaviour of Concrete Confined by Aramid Fibre Spirals', *International Conference on Structural Engineering Mechanics and Computation* pp. 1357–1365.
- Lotfy, M. E. (2010), 'Behaviour of Reinforced Concrete Short Columns with Fiber Reinforced Polymer Bars', *International Journal of Civil and Structural Engineering* **1**(3), 545–557.
- Luca, A. D., Matta, F. & Nanni, A. (2010), 'Behaviour of Full-Scale Glass Fiber-Reinforced Polymer Reinforced Concrete Columns under Axial Load', *ACI Structural Journal* **107**(5), 589–596.
- Mander, J. B., Priestley, M. J. N. & Park, R. (1988), 'Theoretical Stress-Strain Model for Confined Concrete', *ASCE Journal of Structural Engineering* **114**(8), 1804–1826.
- Maranan, G., Manalo, A., Karunasena, K. & Benmokrane, B. (2015), 'Bond Stress-Slip Behaviour: Case of GFRP Bars in Geopolymer Concrete', *ASCE Materials in Civil Engineering* **27**(1), 04014116–1–04014116–8.
- McCaffery, R. (2002), 'Climate Change and the Cement Industry', http://www.ecocem.ie/downloads/Climate_Change_and_the_Cement_Industry.pdf. [Online; accessed March-2015].
- Mohamed, H. M., Affi, M. Z. & Benmokrane, B. (2014), 'Performance Evaluation of Concrete Columns Reinforced Longitudinally with FRP Bars and Confined with FRP Hoops and Spirals under Axial Load', *ASCE Journal of Bridge Engineering* **19**(7), 04014020–1–04014020–12.
- Pessiki, S., Graybeal, B. & Mudlock, M. (2001), 'Proposed Design of High-Strength Spiral Reinforcement in Compression Members', *ACI Structural Journal* **3**(5), 799–810.
- P.K.Mallick (2007), *Fiber-Reinforced Composites: Materials, Manufacturing, and Design, Third Edition*, CRC Press. p. 42.
- Pultrall (2015), 'Fiberglass Reinforcement Building', <http://www.vrod.ca/en/fiberglass-reinforcement-building.asp>. [Online; accessed April-2015].

- Razvi, S. R. & Saatcioglu, M. (1999), 'Circular High-Strength Concrete Columns Under Concentric Compression', *ACI Structural Journal* **96**(5), 817–825.
- Ross, J. D. (2007), 'Analytical Models for Reinforced Concrete Columns with Fiber-Reinforced Polymer Composites', https://kb.osu.edu/dspace/bitstream/handle/1811/25128/undergraduate_thesis.pdf;jsessionid=E68DD034DA2B6ABE44E1DD35DD8DD369?sequence=1. [Online; accessed April-2015].
- Rubber, C. (2015), 'Neoprene Rubber (3.0 X 1200 mm)', <http://www.clarkrubber.com.au/neoprene-rubber-3-0-x-1200mm.html>. [Online; accessed August-2015].
- Sheikh, S. A. & Toklcuc, M. T. (1993), 'Reinforced Concrete Columns Confined by Circular Spirals and Hoops', *ACI Structural Journal* **90**(5), 542–553.
- Tikka, T. (2008), 'Strength of Concrete Columns Reinforced with GFRP Bars', *Australasian Structural Engineering Conference* **93**, 1–10.
- Tobbi, H., Farghaly, A. S. & Benmokrane, B. (2012), 'Concrete Columns Reinforced Longitudinally and Transversally with Glass Fiber-Reinforced Polymer Bars', *ACI Structural Journal* **109**(4), 551–558.
- Wagners (2012), 'Earth Friendly Concrete', <http://www.wagnerscft.com.au/files/2613/4731/0397/Wagners-Earth-Friendly-Concrete.pdf3>. [Online; accessed April-2015].
- Wallah, S. E. & Ramgam, B. V. (2006), 'Low-Calcium Fly Ash-Based Geopolymer Concrete: Long-Term Properties', http://espace.library.curtin.edu.au/cgi-bin/espace.pdf?file=/2008/11/13/file_6/19464. [Online; accessed April-2015].
- Xie, J., Elwi, A. E. & MacGregor, J. G. (1997), 'Performance of High-Strength Concrete Tied Columns: Parametric Study', *ACI Structural Journal* **94**(2), 91–102.
- You, Y., Park, K., Deo, D. & Hwang, J. (2014), 'Tensile Strength of GFRP Reinforced Bars with Hollow Section', <http://www.hindawi.com/journals/amse/aa/621546/>. [Online; accessed April-2015].
- Yu, T. & Teng, J. G. (2011), 'Design of Concrete-Filled FRP Tubular Columns: Provisions in the Chinese Technical Code for Infrastructure Application of FRP Composites', *ASCE Journal of Composites for Construction* **15**(3), 451–461.
- Zeghiche, J. & Chaoui, K. (2005), 'An experimental behaviour of concrete-filled steel tubular columns', *Journal of Constructional Steel Research* **61**(1), 53–66.

Appendix A

Project Specification

University of Southern Queensland
FACULTY OF HEALTH, ENGINEERING AND SCIENCES

ENG4111/4112 Research Project

Project Specification

Topic: **CICRULAR GEOPOLYMER CONCRETE COLUMNS
WITH COMPOSITE REBARS**

For: Matthew Robertson

Supervisor: Dr Allan Manalo

Project Aim: To experimentally investigate the behaviour of 250 mm diameter circular geopolymer concrete columns reinforced with glass fibre reinforced polymer (GFRP) bars under concentric loading

Program: Issue B, 8 March 2015

1. Research the use and parameters of geopolymer concrete and GFRP and their suitability to be used as an alternative to steel reinforced concrete.
2. Investigate, through testing, the effects of different transverse reinforcement types (continuous spiral and circular ties) on the overall strength and behaviour of the specimen.
3. Investigate, through testing, the effect of GFRP ties spacing or pitch on the strength and behaviour of the specimen, as well as analysing the type of failure.
4. Theoretically predict the behaviour of the specimens using equations from existing literature.
5. Submit an academic dissertation on the research, testing and findings.

Agreed:

Student Name: Matthew Robertson

Supervisor Name: Dr Allan Manalo

Examiner: Chris Snook

Date: 8th March 2015

Additional Information

Project Timeline

January 02:	Begin constructing GFRP cages & literature search
February 04:	Have cages in formwork ready for casting
February 05:	Cast geopolymer concrete
February 12:	Remove from formworks
February 18:	Patch any voids within concrete
March 05:	Begin testing of columns
April 1:	Begin write up of results and literature review
May 03:	Begin Preliminary Report
June 03:	Submit Preliminary Report
June 04:	Continue work on thesis
October 29:	Submit thesis

Required Resources

To be sourced through the School of Civil Engineering:

1. Sand
2. Aggregate (varied sized)
3. Cement

Appendix B

Risk Management Plans

**University of Southern Queensland
Risk Management Plan**

Date: 25/02/2015	Faculty/Department: Faculty of Health, Engineering and Sciences	Assessment completed by: <u>Ginghis Maranan</u> Matthew Robertson	Contact number: 0422808442 0400773717
What is the task? Casting and testing of geopolymer concrete columns reinforced with GFRP bars		Location where task is being conducted: P11	
Why is the task being conducted? To investigate the compression behaviour of GFRP reinforced geopolymer concrete columns.			
What are the nominal conditions?			
Personnel Trained personnel / under supervision	Equipment Framed testing machine	Environment Well ventilated controlled temperature	Other
Briefly explain the procedure for this task (including reference to other procedures) Compression test of GFRP reinforced geopolymer columns.			

Risk register and Analysis
 [ALARP - As Low As Reasonably Practicable]

Element or Sub-Element/Process Step	The Risk: What can happen and what will be the results	EXISTING CONTROLS	Risk Rating with existing controls? See next page			Is it ALARP? Yes/No	ADDITIONAL CONTROLS REQUIRED	Risk Rating with additional controls?			Is it ALARP? Yes/No	Risk Decision: Accept/Transfer/Treat
			Consequences	Likelihood	Rating			Consequences	Likelihood	Rating		
List major steps or tasks in process	<ul style="list-style-type: none"> -> Electric shock -> Eye infection -> Fire/explosion -> Physical injury -> Cut/graze Chemical burn 	List all current controls that are already in place or that will be used to undertake the task <ul style="list-style-type: none"> -> List of Personal Protective Equipment (PPE) location -> Identify types facility -> Existing safety measures Existing emergency procedures 	NA	NA	NA	NA	Additional controls may be required to reduce risk rating <ul style="list-style-type: none"> -> Greater containment (FCZ) -> Additional PPE - gloves safety glasses Specific induction / training 	NA	NA	NA	NA	NA
Measuring dimensions of sample	<ul style="list-style-type: none"> - Inhalation of dust - Hand and feet injuries - Falling from the framework - Injuries from incorrect lifting - Electric shock 	<ul style="list-style-type: none"> Wearing of proper Personal Protective Equipments (PPEs) such as safety shoes, gloves, face mask, goggles, and safety harness Use of correct/proper lifting techniques Keep water away from power outlets/cords Risk Management 	NA	NA	NA	NA		NA	NA	NA	NA	NA
Casting of geopolymer concrete			2	C	M	YES	NA	NA	NA	NA	NA	Accept

Element or Sub Element/ Process Step	The Risk: What can happen and what will be the result	EXISTING CONTROLS	Risk Rating with existing controls? See next page			Is it ALARP? Yes/No	ADDITIONAL CONTROLS REQUIRED	Risk Rating with additional controls?			Is it ALARP? Yes/No	Risk Decision: Accept Transfer Treat
			Consequences	Likelihood	Rating			Consequences	Likelihood	Rating		
List major steps or tasks in process	<ul style="list-style-type: none"> - Electric shock - Eye infection - Fire / explosion - Physical injury - Cut / graze - Chemical burn 	List all current controls that are already in place or that will be used to undertake the task eg <ul style="list-style-type: none"> - List of Personal Protective Equipment (PPE) - Identify types facility, location - Existing safety measurers - Existing emergency procedures 	NA	NA	NA	NA	Additional controls may be required to reduce risk rating eg <ul style="list-style-type: none"> - Greater containment (PC2) - Additional PPE – gloves safety glasses - Specific induction / training 	NA	NA	NA	NA	NA
Measuring dimensions of sample	NA	NA	NA	NA	NA	NA	NA	NA	NA	NA	NA	NA
Dismantling of formworks and handling of column specimens	-Hand, feet, and head injuries	Wearing of proper Personal Protective Equipment (PPEs) such as safety shoes, gloves, face mask, hard hats, and goggles Use of overhead crane, forklift, and trolley for lifting and handling the column specimens Risk Management	2	C	M	YES	NA	NA	NA	NA	NA	Accept

<p>Compression test of concrete cylinder and column specimens</p>	<p>-Eye and skin damage due to concrete shattering -Inhalation of concrete debris -Hand and foot injuries due to heavy loads (Potential risk of crushing)</p>	<p>Plan (RMP) has been developed and is readily available. Emergency procedures are in place.</p>	<p>2</p>	<p>YES</p>	<p>Wearing of proper Personal Protective Equipment (PPEs) such as safety shoes, gloves, face mask, hardhat, and goggles Use of overhead crane, forklift, and trolley for lifting and handling the column specimens Standing behind the provided safety wall Risk Management Plan (RMP) has been developed and is readily available. Emergency procedures are in place.</p>	<p>NA</p>																																																										
---	--	--	----------	------------	--	-----------	-----------	-----------	-----------	-----------	-----------	-----------	-----------	-----------	-----------	-----------	-----------	-----------	-----------	-----------	-----------	-----------	-----------	-----------	-----------	-----------	-----------	-----------	-----------	-----------	-----------	-----------	-----------	-----------	-----------	-----------	-----------	-----------	-----------	-----------	-----------	-----------	-----------	-----------	-----------	-----------	-----------	-----------	-----------	-----------	-----------	-----------	-----------	-----------	-----------	-----------	-----------	-----------	-----------	-----------	-----------	-----------	-----------	-----------

USQ RISK RATING ADAPTED FROM A34388:2004

Note: In estimating the level of risk, initially estimate the risk with existing controls and then review risk controls if risk level arising from the risks is not minimal

TABLE 1 - CONSEQUENCE

Level	Descriptor	Examples of Description
1	Insignificant	No injuries. Minor delays. Little financial loss. \$0 - \$4,999*
2	Minor	First aid required. Small spill/gas release easily contained within work area. Nil environmental impact. Financial loss \$5,000 - \$49,999*
3	Moderate	Medical treatment required. Large spill/gas release contained on campus with help of emergency services. Nil environmental impact. Financial loss \$50,000 - \$99,999*
4	Major	Extensive or multiple injuries. Hospitalisation required. Permanent severe health effects. Spill/gas release spreads outside campus area. Minimal environmental impact. Financial loss \$100,000 - \$250,000*
5	Catastrophic	Death of one or more people. Toxic substance or toxic gas release spreads outside campus area. Release of genetically modified organism (s) (GMO). Major environmental impact. Financial loss greater than \$250,000*

* Financial loss includes direct costs eg workers compensation and property damage and indirect costs, eg impact of loss of research data and accident investigation time.

TABLE 2 - PROBABILITY

Level	Descriptor	Examples of Description
A	Almost certain	The event is expected to occur in most circumstances. Common or repetitive occurrence at USQ. Constant exposure to hazard. Very high probability of damage.
B	Likely	The event will probably occur in most circumstances. Known history of occurrence at USQ. Frequent exposure to hazard. High probability of damage.
C	Possible	The event could occur at some time. History of single occurrence at USQ. Regular or occasional exposure to hazard. Moderate probability of damage.
D	Unlikely	The event is not likely to occur. Known occurrence in industry. Infrequent exposure to hazard. Low probability of damage.
E	Rare	The event may occur only in exceptional circumstances. No reported occurrence globally. Rare exposure to hazard. Very low probability of damage. Requires multiple system failures.

TABLE 3 – RISK RATING

Probability	Consequence				
	Insignificant 1	Minor 2	Moderate 3	Major 4	Catastrophic 5
A (Almost certain)	M	H	E	E	E
B (Likely)	M	H	H	E	E
C (Possible)	L	M	H	H	H
D (Unlikely)	L	L	M	M	M
E (Rare)	L	L	L	L	L

TABLE 4 - RECOMMENDED ACTION GUIDE

Abbrev	Action Level	Descriptor
E	Extreme	The proposed task or process activity MUST NOT proceed until the supervisor has reviewed the task or process design and risk controls. They must take steps to firstly eliminate the risk and if this is not possible to introduce measures to control the risk by reducing the level of risk to the lowest level achievable. In the case of an existing hazard that is identified, controls must be put in place immediately.
H	High	Urgent action is required to eliminate or reduce the foreseeable risk arising from the task or process. The supervisor must be made aware of the hazard. However, the supervisor may give special permission for staff to undertake some high risk activities provided that system of work is clearly documented, specific training has been given in the required procedure and an adequate review of the task and risk controls has been undertaken. This includes providing risk controls identified in Legislation, Australian Standards, Codes of Practice etc.* A detailed Standard Operating Procedure is required, and monitoring of its implementation must occur to check the risk level.
M	Moderate	Action to eliminate or reduce the risk is required within a specified period. The supervisor should approve all moderate risk task or process activities. A Standard Operating Procedure or Safe Work Method statement is required.
L	Low	Manage by routine procedures.

*Note: These regulatory documents identify specific requirements/controls that must be implemented to reduce the risk of an individual undertaking the task to a level that the regulatory body identifies as being acceptable.

The task should not proceed if the risk rating after the controls are implemented is still either HIGH or EXTREME or if any risk is not As Low As Reasonably Practicable (ALARP).

This Risk Assessment score of Low (L) is only on the condition that all existing and additional controls are in place at the time of the task being conducted.

Assessment completed by:	
Name: Ginghis Marapan Matthew Robertson	Signature:
Position: PhD Student Undergraduate Student	Contact No: 0422808442 0400773717
Date: 25/02/2015	
Supervisor	
Dr Allan Manalo	Signature:
Position : Senior Lecturer, FoHES	Contact No:
Date:	

Guidance Notes for review of Controls and Risk Management Plan.

When monitoring the effectiveness of **control measures**, it may be helpful to ask the following questions:

- **Have the chosen control measures been implemented as planned?**
 - Are the chosen control measures in place?
 - Are the measures being used?
 - Are the measures being used correctly?
- **Are the chosen control measures working?**
 - Have any the changes made to manage exposure to the assessed risks resulted in what was intended?
 - Has exposure to the assessed risks been eliminated or adequately reduced?
 - **Are there any new problems?**
 - Have the implemented control measures introduced any new problems?
 - Have the implemented control measures resulted in the worsening of any existing problems?

To answer these questions:

- consult with workers, supervisors and health and safety representatives;
- measure people's exposure (e.g. taking noise measurements in the case of isolation of a noise source);
- consult and monitor incident reports; and
- review safety committee meeting minutes where possible.

Set a date for the review of the **risk management process**. When reviewing, check if:

- the process that is currently in place is still valid;
- things have changed that could make the operating processes or system outdated;
- technological or other changes have affected the current workplace; and
- a different system should be used altogether

Appendix C

Instrumentation Used During Testing

This appendix provides a picture of all the instrumentation listed in chapter 3. These items included:

- 1x Hydraulic Jack
- 1x Circular Steel Plate $\phi 285\text{mm}$
- 4x Steel Bands
- 2x Neoprene Rubber 300x300x3mm
- 2x Neoprene Rubber 800x300x3mm
- 1x Square Steel Plate
- 1x Load Cell
- 1x Rectangular Steel Plate
- 1x Stringpot
- 2x Lasers
- 1x Aviary Wire 1400x900mm
- 1x Computer with the System 5000 program installed
- 1x Video Camera



Figure C.1: The 2000kN hydraulic jack used.



Figure C.2: The circular plate used to evenly distribute the load.



Figure C.3: The neoprene rubber used.

(Rubber 2015)



Figure C.4: The steel plate that was used.



Figure C.5: The load cell used.



Figure C.6: The base plate used.



Figure C.7: The stringpot used to measure deflection.

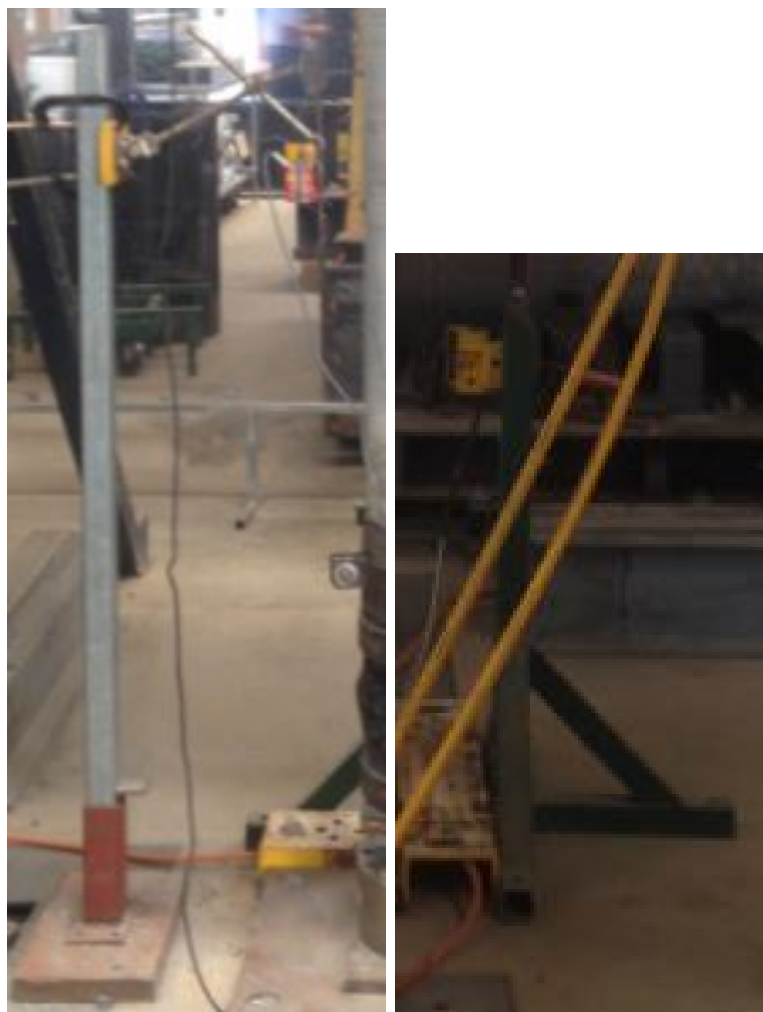


Figure C.8: The lasers used to measure the mid span expansion.



Figure C.9: The aviary wire used to control shattered concrete.

(Improvement 2015)



Figure C.10: The computer used to log all recorded data.